

NUMERICAL STUDY OF DOUBLE DIFFUSIVE MIXED CONVECTIVE PHENOMENA IN A SQUARE ENCLOSURE

**THESIS SUBMITTED IN PARTIAL FULFILMENT OF THE
REQUIREMENT FOR DEGREE OF MASTER OF ENGINEERING IN
MECHANICAL ENGINEERING UNDER
FACULTY OF ENGINEERING AND TECHNOLOGY**

Submitted by

CHANDAN KUMAR YADAV

Class Roll No.: 002011202031

Registration No.: 154329 of 2020-21

Exam Roll No.: M4MEC22030

Academic Session: 2020-2022

Under the guidance

of

Prof. Nirmal Kumar Manna

**Department of Mechanical Engineering
Jadavpur University, Kolkata – 700032**

and

Asst. Prof. Nirmalendu Biswas

**Department of Power Engineering
Jadavpur University, Kolkata – 700106**

**DECLARATION OF ORIGINALITY AND COMPLIANCE OF
ACADEMIC ETHICS**

I hereby declare that the thesis entitled “**NUMERICAL STUDY OF DOUBLE DIFFUSIVE MIXED CONVECTIVE PHENOMENA IN A SQUARE ENCLOSURE**” contains a literature survey and original research work by the undersigned candidate, as a part of his *MASTER OF ENGINEERING IN MECHANICAL ENGINEERING* under the *DEPARTMENT OF MECHANICAL ENGINEERING*, studies during academic session 2020-2022.

All information in this document has been obtained and presented in accordance with the academic rules and ethical conduct.

I also declare that, as required by these rules of conduct, I have fully cited and referenced all the material and results that are not original to this work.

Name: **CHANDAN KUMAR YADAV**

Class Roll Number: **002011202031**

University Registration No: **154329 of 2020-21**

Examination Roll No: **M4MEC22030**

Date:

Signature:

**FACULTY OF ENGINEERING & TECHNOLOGY
DEPARTMENT OF MECHANICAL ENGINEERING
JADAVPUR UNIVERSITY
KOLKATA-700032**

CERTIFICATE OF RECOMMENDATION

This is to certify that the thesis entitled “**NUMERICAL STUDY OF DOUBLE DIFFUSIVE MIXED CONVECTIVE PHENOMENA IN A SQUARE ENCLOSURE**” is a bonafide work carried out by **CHANDAN KUMAR YADAV** under our supervision and guidance in partial fulfilment of the requirements for awarding the degree of Master of Engineering in Mechanical Engineering under Department of Mechanical Engineering, Jadavpur University during the academic session, 2020-2022.

THESIS SUPERVISOR
Prof. Nirmal Kumar Manna
Department of Mechanical
Engineering
Jadavpur University, Kolkata

THESIS SUPERVISOR
Asst. Prof. Nirmalendu Biswas
Department of Power
Engineering
Jadavpur University, Kolkata

Prof. Chandan Mazumdar
Dean
Faculty Council of Engineering
and Technology
Jadavpur University, Kolkata

Prof. Amit Karmakar
Head of Department
Department of Mechanical
Engineering
Jadavpur University, Kolkata

**FACULTY OF ENGINEERING & TECHNOLOGY
DEPARTMENT OF MECHANICAL ENGINEERING
JADAVPUR UNIVERSITY
KOLKATA-700032**

CERTIFICATE OF APPROVAL

The foregoing thesis, entitled “**NUMERICAL STUDY OF DOUBLE DIFFUSIVE MIXED CONVECTIVE PHENOMENA IN A SQUARE ENCLOSURE**” is hereby approved as a creditable study in the area of Mechanical Engineering carried out and presented by **CHANDAN KUMAR YADAV** in a satisfactory manner to warrant its acceptance as a prerequisite to the degree for which it has been submitted. It is notified to be understood that by this approval, the undersigned do not necessarily endorse or approve any statement made, opinion expressed and conclusion drawn therein but approve the thesis only for the purpose for which it has been submitted.

**Committee of the final evaluation
of the thesis:**

Signature of Examiners

ACKNOWLEDGEMENT

At first, I would like to express my thankfulness and gratitude to my supervisor, Professor Nirmal Kumar Manna for his valuable guidance and suggestions throughout my thesis work. I am very much indebted to him for giving me the opportunity to pursue my M. Tech thesis work under his guidance. Without his precious knowledge in the field of Fluid Mechanics and Heat Transfer especially the CFD domain, my project work would not have taken a meaningful shape. I have learned quite a lot about the COMSOL MULTIPHYSICS simulation software package without which the development of my M. Tech project would have been very tough. I will be benefited throughout my life from the knowledge that I gained here under his enormous guidance.

I also extend my thanks and appreciation towards my co-supervisor, Assistant Professor Nirmalendu Biswas of Dept. of Power Engineering, Jadavpur University, for extensively guiding me during my thesis work. He has always encouraged and supported me to get my work published in various conferences.

Finally, I thank my parents who have always supported me with deep love and sacrifice throughout my life. I pray for their happiness and good health, and I dedicate my work to them in the sincerest way I can think of.

(Chandan Kumar Yadav)

ABSTRACT

Double diffusion convection is a complex heat and mass transfer mechanism where the density change is governed by both temperature and concentration differences. This phenomenon is widely noticed in the distinct natural and real processes, various disciplines of science and engineering, and several industries like oceans, transfer of contaminant/moisture in air, H₂O and soil, geology, biotechnology, heat exchangers, thermal insulations, electronic equipment, solar collectors, drying process, manufacturing of crystal and so on. In view of this, the current study deals with the combined heat and mass transfer within a square domain comprising of steady, laminar, and mixed convective flow of H₂O (Pr = 5.83); subjected to differential heating and concentration boundary conditions together with the non-magnetic (Ha = 0) and the magnetic effects. This work is numerically conducted by considering Galerkin's finite element technique and the same is utilized to discretize the relevant governing transport equations which are considered in the non-dimensional form for the present simulation. Here, the solution results are explained through a broad range of variations of dimensionless numbers such as Reynolds number ($= 10 \leq Re \leq 100$), Richardson number ($= 0.1 \leq Ri \leq 10$), Lewis number ($= 1 \leq Le \leq 5$), Buoyancy ratio ($= -10 \leq N \leq 10$), and Hartmann number ($= 0 \leq Ha \leq 80$) and their pertinent effects of variation are highlighted through the various visualization plots such as Streamlines, Isotherms, Iso-concentration curves, Heatlines, Nu_{avg} and Sh_{avg} to recognize the fluid flow field along with the thermo-solute transport process within the enclosure. Further to that, this numerical examination implies the parametric conditions for which heat and species transfer inside the cavity tend towards the optimization. Quantitatively, it is established that optimum thermal transport phenomena within the enclosure is attained under the parametric conditions of $Re = 100$, $Ri = 0.1$, $Le = 1$, $N = 1$, and $Ha = 0$ for which $Nu_{avg} = 5.5381$. Also, the optimum species transfer within the cavity is achieved for the parameters $Re = 50$, $Ri = 0.1$, $Le = 5$, $N = 1$, and $Ha = 0$ leading to $Sh_{avg} = 5.4501$.

List of Figures

- Fig. 2.1:** Schematic Diagram for the Considered Problem Geometry (a) Absence of the Magnetic Field and (b) Presence of the Magnetic Field.
- Fig. 2.2:** Block Diagram Representation of the Solution Technique using FEM
- Fig. 2.3:** Comparison of the present FEM code with the Al-Amiri work.
- Fig. 3.1:** Streamline Contours for $N = 1$, $Le = 1$ at $Ha = 0$.
- Fig. 3.2:** Isotherm Plots for $N = 1$, $Le = 1$ at $Ha = 0$.
- Fig. 3.3:** Concentration Curves for $N = 1$, $Le = 1$ at $Ha = 0$.
- Fig. 3.4:** Heat lines for $N = 1$, $Le = 1$ at $Ha = 0$.
- Fig. 3.5:** Streamline Contours for $Re = 50$, $N = 1$ at $Ha = 0$.
- Fig. 3.6:** Isotherm Plots for $Re = 50$, $N = 1$ at $Ha = 0$.
- Fig. 3.7:** Concentration Curves for $Re = 50$, $N = 1$ at $Ha = 0$.
- Fig. 3.8:** Heat lines for $Re = 50$, $N = 1$ at $Ha = 0$.
- Fig. 3.9:** Streamline Contours for $Re = 10$, $Le = 1$ at $Ha = 0$.
- Fig. 3.10:** Isotherm Plots for $Re = 10$, $Le = 1$ at $Ha = 0$.
- Fig. 3.11:** Concentration Curves for $Re = 10$, $Le = 1$ at $Ha = 0$.
- Fig. 3.12:** Heat lines for $Re = 10$, $Le = 1$ at $Ha = 0$.
- Fig. 3.13:** Streamline Contours for $Re = 100$, $Le = 1$, and $N = 1$.
- Fig. 3.14:** Isotherm Plots for $Re = 100$, $Le = 1$, and $N = 1$.
- Fig. 3.15:** Concentration Curves for $Re = 100$, $Le = 1$, and $N = 1$.
- Fig. 3.16:** Heat lines for $Re = 100$, $Le = 1$, and $N = 1$.
- Fig. 3.17:** Variation of Average Nu with Re and Ri for $Le = 1$, $N = 1$, $Ha = 0$.
- Fig. 3.18:** Variation of Average Sh with Re and Ri for $Le = 1$, $N = 1$, $Ha = 0$.
- Fig. 3.19:** Variation of Average Nu with Le and Ri for $N = 1$, $Re = 50$, $Ha = 0$.
- Fig. 3.20:** Variation of Average Sh with Le and Ri for $N = 1$, $Re = 50$, $Ha = 0$.
- Fig. 3.21:** Variation of Average Nu with N and Ri for $Le = 1$, $Re = 10$, $Ha = 0$.
- Fig. 3.22:** Variation of Average Sh with N and Ri for $Le = 1$, $Re = 10$, $Ha = 0$.
- Fig. 3.23:** Variation of Average Nu with Ha and Ri for $Le = 1$, $N = 1$, $Re = 100$.
- Fig. 3.24:** Variation of Average Sh with Ha and Ri for $Le = 1$, $N = 1$, $Re = 100$.

List of Publications

- 1) C.K. Yadav, K. Dey, N.K. Manna, N. Biswas, Low Reynolds number MHD mixed convection of nanofluid in a corner heated grooved cavity, *Materials Today: Proceedings*, (2022), <https://doi.org/10.1016/j.matpr.2022.02.443>.
- 2) C.K. Yadav, A. Halder, S. Mukherjee, N.K. Manna, N. Biswas, D.K. Mandal, Effect of sinusoidal heating and Hartmann number on nano-fluid based heat flow evolution in a cavity, *Materials Today: Proceedings*, <https://doi.org/10.1016/j.matpr.2022.02.434>.
- 3) C.K. Yadav, N.K. Manna, N. Biswas, D.K. Mandal, MHD Flow of Nano liquid within a Recto-triangular Geometry having Bottom heating, *ICFTES 2022 (The 1st International Conference in Fluid, Thermal, and Energy Systems)*, 9th - 11th June 2022, NIT Calicut, Kerala, India.

NOMENCLATURE

B	magnetic field ($\text{N A}^{-1} \text{m}^{-2}$)
g	acceleration due to gravity (m s^{-2})
H	cavity height (m)
W	cavity depth (m)
A	cavity aspect ratio
Ha	Hartmann number
p	dimensional pressure (Pa)
P	dimensionless pressure
Pr	Prandtl number
Le	Lewis number
Nu_{avg}	average Nusselt number
Sh_{avg}	average Sherwood number
Ri	Richardson number
Re	Reynolds number
N	Buoyancy ratio
T	dimensional temperature (K)
x, y	dimensional coordinate axes
X, Y	nondimensional coordinate axes
u, v	dimensional velocity components (ms^{-1})
U, V	nondimensional velocity components
θ	nondimensional temperature
C	nondimensional concentration
ρ	density (kg m^{-3})
ν	kinematic viscosity ($\text{m}^2 \text{s}^{-1}$)
β_T	thermal expansion coefficient (K^{-1})
β_S	solubility expansion coefficient
α	thermal diffusivity ($\text{m}^2 \text{s}^{-1}$)
D	mass diffusivity ($\text{m}^2 \text{s}^{-1}$)

CONTENTS

Chapter 1: Overview of the Work

- 1.1 Introduction
- 1.2 Literature Survey
- 1.3 Inspiration and Purpose behind the Work
- 1.4 Structure of the Work

Chapter 2: Mathematical Modelling and Numerical Technique

- 2.1 Physical Description of the Problem
- 2.2 Numerical Technique
- 2.3 Validation Study

Chapter 3: Results and Discussion

- 3.1 Effect of Richardson and Reynolds Numbers
- 3.2 Effect of Richardson and Lewis Numbers
- 3.3 Effect of Richardson Number and Buoyancy Ratio
- 3.4 Effect of Richardson and Hartmann Numbers
- 3.5 Heat and Mass Transfer Characteristics
- 3.6 Conclusions

Chapter 4: Scope of Future Work

References

CHAPTER – 1

Overview of the Work

1.1 Introduction

Dual diffusion-based convection is a thermo-solute transport mechanism where fluid motion is caused due to the combined action of thermal and concentration buoyant forces produced by respective changes in temperature and concentration. Here, variation of density is ruled by the temperature as well as concentration gradients. Fluid flow under this situation is significantly affected by the relative magnitudes of thermal and concentration buoyant forces. A literature survey reveals that in recent years, several researchers have analyzed the combined heat and mass transfer process both experimentally and theoretically. However, most of the studies are numerical based because of involved process complexities. This phenomenon is frequently observed in the different natural processes, multiple engineering fields, and various industries like oceans, lakes, ambient, transfer of contaminant/moisture in the air, H₂O and soil, pollutant transfer in ground water, geology, medical (cancer-treatment), biotechnology, astrophysics, heat exchangers, removal and storage of heat, thermal insulations, cold storage and refrigeration systems, electronic equipment, cryogenics, MEMS, multi-shield structures in case of nuclear reactors, furnaces, solar collectors and ponds, printing, drying process, food processing, chemical processing equipment, manufacturing of crystal, glass production, solidification of alloys, petrochemical processes, cooling and heating of buildings, storage and transport of liquefied natural gas, buildings ventilation system design and so on.

Double diffusive natural (gravity-induced) and mixed (lid-driven flow) convective flows within a cavity are frequently experienced and studied due to their wide range of applications in distinct kinds of geometries such as rectangle, square, triangle, trapezoidal, spherical, cylindrical, ellipsoidal, sinusoidal, and so on.

Double diffusion free convection is established due to cumulative temperature and compositional gradients. It is a very popular thrust area associated with the thermo-fluidic study. As per the literature, combined heat and mass transport processes involving buoyancy-induced cavity flow have been investigated by many investigators in recent decades because of their wide range of environmental, scientific, engineering, and industrial uses such as atmosphere, pollutant transport

(within H₂O, Air and soil), ocean currents, lakes, geo-science, astrophysics, chemistry, biology, double pane windows, solar ponds and collectors, printing, energy storage devices, heat exchangers, chemical and nuclear reactors, the process of drying, storage of food, sterilization, material processing, casting-solidification, metallurgy, fabrication of semi-conductor devices utilizing the crystal growth process, storage tanks for natural gas, ventilation of home, cabins of aircraft, etc.

Thermo-solute free convection plays a significant role in the growth of crystals where it influences temperature and concentration of fluid at the interface of phase leading to a unit crystal of poor quality because of the turbulence effect. The process of solidification in a binary alloy is significantly affected by this process. Crystal growth serves as the basis for the manufacturing of electronic appliances and equipment such as infrared detectors, transistors, memory and microwave devices, and ICs.

Double diffusion hybrid convection is a complex flow phenomenon happening due to the joint effect of shear-induced flow and temperature-concentration gradient leading to buoyancy-induced flow. In such context, flow in a differentially heated or cooled lid-driven geometry is a necessary and extremely familiar arrangement. The mixed convection process having thermo-solute transport has been examined by multiple authors in the last few decades; as this process finds numerous applications in practical engineering and industrial processes such as heat exchangers, spray and flash drying, dehydration and drying processes in food and chemical processing plants, atomized liquid fuels combustion, material processing, contaminant transport, separation process, evaporation of cyclone, etc.

In the process of drying, thorough knowledge regarding the physics involved is essential for the efficient operation of the drying equipment. Here, the presence of both temperature and compositional gradients leads to intricate flow configurations within the drying container and subsequently enables the possible moisture transport. A conventional drying system may be considered as a cavity such that its lower surface is subjected to heating to ensure the liquid solvent evaporation, whereas the upper surface is kept cold for the condensation of vapor solvent at that place. Ultimately, mechanical material handling namely belt conveyor is used to eliminate the unwanted moisture or contaminants.

1.2 Literature Survey

The double-diffusive convective transport process involves many complexities because of the impact of different factors such as mixed flow regime, complicated geometry shapes, MHD and nanofluid flow, distinct heating-concentration conditions, and porous media, non-Newtonian fluid flow, etc. The effects of each of the elements on simultaneous heat and mass transfer are presented and discussed subsequently in detail through the extensive studies carried out by multiple researchers.

Over the last few decades, lots of works have been carried out on lid-driven cavity flow including thermo-solute transport by various authors. In this context, Al-Amiri et al. [1] conducted a numerical study on the laminar double-diffusive mixed convective flow of a binary fluid inside a square lid-driven cavity by using the Galerkin's finite element technique. It is found that heat transfer (average Nusselt number Nu_{avg}) and mass transfer (average Sherwood number Sh_{avg}) characteristics inside the geometry are enhanced under the conditions of the low value of Richardson number $Ri = 0.01$ and high value of buoyancy ratio $N = 100$ at Lewis number $Le = 1$. Steady double diffusion mixed convection within a rectangular enclosure was numerically inspected by Teamah and El - Maghlany [2] with the aid of the finite volume code. They observed that heat and mass transfer rate both increase with the reduction in Ri value and increment in the positive value of N . Teamah et al. [3] numerically reported for the double diffusive-mixed convective flow of H_2O in an inclined geometry. This work aims to observe and analyze the tilting effect of the cavity on the flow, thermal and mass fields.

Free convective heat and mass transfer mechanism inside numerous geometries of regular shapes like square, rectangle, parallelogram, triangle, trapezoidal, rhomboidal, cubic, cylindrical, spherical, ellipsoidal, etc. has been extensively examined by several researchers in the last few years due to enhanced requirement of the heat and mass transfer in practical applications. Qin et al. [4] have used finite difference approach to perform the study of double diffusion natural convection mechanism inside a rectangular enclosure with differential temperature-concentration effect. It is noticed that the average Nusselt number (avg. Nu) diminishes with the increment of Le for $Le < 0.35$ and enhances for the increase of Le with $Le > 0.35$. However, the avg. Sh rises every time with the increase of Le . Chen et al. [5] have mathematically investigated for the unsteady double diffusion and

turbulent free convective flow in square geometry by the help of the lattice Boltzmann model. Rahman et al. [6] have numerically worked for a solar collector of isosceles triangle shape having the double-diffusion free convective flow of air by using Galerkin's finite-element approach. It was noted that both heat and mass transport rises with an increment of the Rayleigh number and buoyancy ratio. Corcione et al. [7] have performed numerical simulation on unsteady double diffusion and laminar free convection by taking a 2-D square cavity involving a binary fluid. Nazari et al. [8] have utilized the lattice Boltzmann technique of numerical investigation for the double diffusion free convection by considering a square geometry having warm obstruction of square configuration. The outcome of this work is that both Nu_{avg} and Sh_{avg} enhance for the increment of Rayleigh number and cavity aspect ratio. Koufi et al. [9] have worked on steady heat and species transfer process involving the laminar free convective flow of either Air or Air-CO₂ within a differentially heated square geometry by employing the finite volume technique. Arun et al. [10] have conducted the numerical study by utilizing the lattice Boltzmann technique for combined heat and mass transfer problems involving steady buoyancy-induced laminar convection within a computational domain having an open end at the right side. The study reveals that both Nu_{avg} and Sh_{avg} enhance with the increment of aspect ratio. Said et al. [11] have numerically computed by using ANSYS Fluent CFD software for the thermo-solute free convective phenomena along with entropy evolution within a differentially heated -concentrated square-shaped enclosure comprising of air-CO₂ binary mixture under a turbulent flow regime. It is observed that entropy generation is significantly affected by N and it tends to be minimum for $N = -1$ at a higher value of the thermal Rayleigh number.

Actual life problems frequently deal with the complicated shapes, irregular sizes and sinusoidal configurations of enclosures. Thus, in recent days various authors have concentrated towards the study of the thermo-solute buoyancy-induced convective flow phenomena within such typical cavities. In this connection, Ghernoug et al. [12] have considered a horizontal eccentric annulus which is a cylinder in shape for the numerical estimation of steady double diffusion and laminar free convective phenomena. Here, the interior and exterior walls of the cylinder are at high and low temperature-concentration effects respectively. Taloub et al. [13] have numerically computed with the help of Patankar's finite-volume technique through consideration of a special kind of geometrical annulus passage formed by two horizontal elliptic

cylinders involving double diffusion and laminar free convective flow of air. It is reported that both Nu_{avg} and Sh_{avg} enhance with an increment of the thermal Rayleigh number. Al-Farhany et al. [14] have performed numerical research by using the Galerkin's technique of finite-element for the combined heat and mass transfer process involving the steady, free, and laminar convective flow of moist air within a complicated 2-D enclosure configured in a staggered way having two obstacles in equi-triangle form. This study reveals that both Nu_{avg} and Sh_{avg} reduce when the inner triangle size is increased. It is observed that highest successive decline of Nu_{avg} and Sh_{avg} is 15.3% and 5.1% for the rise of triangle size at fixed magnitudes of $Ra = 10^6$ and $Le = N = 4$. Eshaghi et al. [15] have carried out numerical analysis with the aid of a finite element approach for the steady double diffusion buoyancy-induced laminar convective flow of Cu-Al₂O₃-H₂O based nano-fluid within a typical geometry of H-shape having an inside baffle placed at the upper surface. This study implies that enhancement in Nu_{avg} occurs by 0.1% for variation of baffle orientation from 0° to -60°; whereas improvement in Sh_{avg} occurs by 0.2% for a change of baffle orientation from 0° to +60°.

Magneto-hydrodynamics (MHD) is the branch of fluid mechanics dealing with the action of an external magnetic field on fluid motion. Magnetic field acts as a significant damping agent to regulate the convective fluid flow involving heat and species transport within geometries of practical interest. This is since Lorentz force produced in a translating fluid by the application of a magnetic field reduces the fluid motion, flow strength, and hence associated heat-mass transfer. The magnetic field intensity is given by the Hartmann number (Ha) and the increment in Ha results into rise of the Lorentz force magnitude. MHD effect is widely observed in manufacturing sectors and engineering problems such as metal processing, casting of metal, growth of crystal, micro and nano-electronic systems (miniaturization purpose), food-processing, drying industries, thermal insulations, cooling of nuclear reactors, Petrochemical industries, cavity-based flow, flow of jet, geothermal energy reservoirs, bio-medical (plasma therapy), and so on. Fluid flow pattern along with temperature-concentration at the time of solidification in case of casting and crystal growth is controlled by the exposure of magnetic field.

Henceforth, double diffusion MHD convective flow together with entropy generations within enclosures has been largely investigated by researchers as a key research domain in recent times. In view of the same, Moolya and Satheesh [16] have

considered a lid-driven inclined rectangular geometry with differential heating-concentration effect for numerical analysis of the double-diffusive mixed and MHD convective flow. It is concluded that both Nu and Sh increase with the increment of cavity inclination and they decrease with the increase of Hartmann number. Also, the optimum value of cavity tilt is 60° for $N = 1$ and it is 30° at $N = -1$ to obtain improved heat and mass flow. Moolya and Anbalgan [17] have considered an inclined rectangular cavity for numerical analysis of the double-diffusion steady and mixed MHD convection flow problem by using the finite volume method. This work reveals that maximum heat ($Nu_{avg} = 27.35$) and optimum mass transfer ($Sh_{avg} = 34.79$) are attained under the conditions of $Ri = 10$, $Ha = 0$, and $Pr = 7$ when cavity orientation is 60° . Teamah and Shehata [18] have carried out a numerical study with the aid of the finite volume technique for the steady double-diffusion free convection mechanism inside a 2-D trapezoidal cavity with various inclination angles and imposed to magnetic effects in a horizontal direction. Here the geometry is chosen such that its bottom wall is warmer having high concentration, inclined walls are colder with low concentration, and the remaining top wall is taken as to be insulated and impermeable. Maatki, Ghachem et al. [19] have conducted a numerical study on thermo-solute free MHD convection inside a 3-D cubical enclosure having binary fluid. The outcome of this investigation is that the flow within the cavity gets reduced with an increment of the magnetic field inclination. Maatki et al. [20] have used the finite volume code for numerical analysis of the steady double diffusive and laminar free convective flow of a binary mixture by considering a 3-D cavity in cubic shape under impacts of magnetic field. The motive of this work is to estimate the entropy generation within the enclosure. This study reveals that entropy evolution rises with increment in Ha and subsequently, it becomes homogeneous throughout the geometry. Mondal and Sibanda [21] have reported numerically by using the finite-difference technique for the transient state double diffusive and MHD free convective flow of air inside an oriented rectangular cavity.

Reddy and Murugesan [22] have performed numerical investigation by using Galerkin's finite-element approach for the MHD free convective flow together with heat and mass transport inside a square enclosure subjected to differential temperature-concentration effect. In this study, they have used different working substances such as Gallium, H_2O , and gas. Transient thermo-solute and free laminar convective flow of H_2O within a square geometry imposed to the magnetic field is

mathematically computed with the help of MATLAB code by the Venkatadria et al. [23]. All wall surfaces of the enclosure are adiabatic and impermeable except the left one having uniformly heated and concentrated. Sathiyamoorthi and Anbalagan [24] have adopted the lattice Boltzmann method for numerical computation of the double diffusion free convection mechanism inside an oriented geometry subjected to a magnetic field. This work tells that effect of geometry inclination is significant at a large Ra value. Mahapatra and Mondal [25] have utilized the finite difference technique of numerical investigation for the combined heat and mass transfer along with steady buoyant convection within a 2-D trapezoidal-shaped cavity subjected to the magnetic field impact. The primary purpose of this work is to perform heat and mass line analysis with a distinct cavity aspect ratio. Mojumder et al. [26] have used the Galerkin's weighted residual iterative approach of finite element for the numerical investigation of steady double diffusion and laminar free MHD convective phenomena inside a differentially heated-concentrated square-shaped enclosure having cylindrical isothermal obstruction internally located at the very middle of the geometry. They have carried out parametric investigation in terms of the Ha ($= 0 - 50$), Le ($= 1 - 20$), and Buoyancy ratio ($N = -5$ to 5) at $Pr = 0.71$ and $Ra = 10^4$.

It is the low thermal conductivity value of conventional fluids (H_2O , air, oil, glycerol, engine oil, ethylene glycol and so on); which enables their limited use for the engineering and industrial applications requiring enhanced heat transfer (cooling) performance. Investigators are largely focused to increase the thermal transport phenomena by inventing new techniques. In such a context, nanofluid technology plays a significant role. The term 'nano liquid' was very first introduced by Choi. Nanofluids have higher effective thermal conductivity as compared to the base fluids and subsequently, their employment result in enhanced heat transfer of thermal functioning systems. They are formed by mixing pure metals and their oxides as nanoparticles (size: $1 - 100$ nm) such as Ag, Cu, CuO, Al, Ni, Al_2O_3 , Fe_2O_3 , TiO_2 , etc. within carrier fluids. Solid nanoparticles usually consist of three layers namely surface, core, and shell. The thermal transport features of these smart fluids are primarily affected by the thermos-physical behaviors of the nanoparticles and the traditional fluid together with size, shape, and volumetric concentration of nanoparticles. Sometimes hybrid nanofluids are considered and they are developed by adding two distinct solid nanoparticles within the conventional fluid. In such a context, Cu- Al_2O_3 is frequently adopted by the investigators. Nowadays, nanofluids

are employed in a significant manner for industrial utilities and engineering purposes like electronic equipment cooling, refrigerants, heat exchangers, nuclear reactors, material science, bio-medical and chemical field, microfluidics, fuel cells, solar devices and systems (solar cells, solar heaters and collectors) and many more.

Dual-diffusion convective flow of nanofluids is an interesting subject of research. In recent years, multiple works have been carried out by various investigators for the combined heat and mass transport phenomena involving a buoyancy-induced convective flow of nanofluids within distinct enclosures as a thrust research area. In this connection, double-diffusion laminar mixed convection of $\text{Al}_2\text{O}_3\text{-H}_2\text{O}$ nanofluid in a 2-D trapezoidal enclosure subjected to a vertical magnetic field is numerically studied with the aid of the finite difference method by Mondal and Mahapatra [27]. The sole aim of this work is to minimize the entropy generation. It was found that entropy generation is minimum at low value of Ha and cavity aspect ratio, especially at lower $Ri = 0.01$. Shah et al. [28] have numerically reported for the steady double-diffusive and mixed convective laminar flow of nanofluid within a trapezoidal geometry involving an obstacle (cold) in elliptic form. In this work, transport equations are solved by considering the finite-element technique using Galerkin's weighted residual iterative approach. Esfahani and Bordbar [29] have adopted the finite-volume methodology for numerical investigation of the double-diffusive steady and laminar natural convective flow phenomena of water-based nanofluid within a square geometry subjected to differential heating and concentration. Here, different nanoparticles (Ag, Cu, Al_2O_3 , TiO_2) are used for the analysis purpose. This work implies that optimum heat transfer is attained for Ag particles. Sheikhzadeh et al. [30] have numerically worked for $\text{Al}_2\text{O}_3\text{-H}_2\text{O}$ nano-fluid flow inside a square cavity involving double diffusion free convection mechanism by using the finite-volume technique together with the SIMPLER algorithm. Chen et al. [31] have used the lattice Boltzmann methodology for the numerical examination of the unsteady double-diffusive and free convective flow of $\text{SiO}_2\text{-H}_2\text{O}$ nano-fluid within a rectangular enclosure. This work concludes that entropy generation decreases with the increment in nanoparticle concentration. Free convection involving heat and species transfer within a geometry of window like shape having three obstructions in form of square along with the nanofluid flow has been mathematically investigated with the aid of Galerkin's finite-element approach by Chowdhury et al. [32]. They have utilised different nanoparticles like Ag, Cu, Al_2O_3 along with H_2O for the

investigation purpose and reported that thermo-solute transfer is optimum when Ag is used as the nanoparticle along with the carrier fluid H₂O. Abidi et al. [33] have used the finite-volume technique for the combined heat and mass transport process within a 3-D cubic domain involving free convective flow of micro polar Al₂O₃-H₂O nanofluid subjected to the hydro-magnetic impact. The study reveals that both heat and species transfer get diminish at Ha = 0 and they tend to improve for Ha > 30 with the addition of the nanoparticles.

Ali et al. [34] have used Galerkin's finite element method for numerically analyzing the combined heat and mass transfer process involving the steady laminar free convective flow of Cu-H₂O nanofluid within a square geometry under the MHD effect. Steady double diffusion laminar free convection of H₂O-based nanofluid using Cu, Ag, Al₂O₃, TiO₂ as distinct nanoparticles inside a trapezoidal geometry imposed to the magnetic field effect is numerically examined with the help of the finite-difference technique by Mahapatra et al. [35]. They have observed that the thermo-solute phenomena tend to be maximum for Ag and Cu nanoparticles. Saha et al. [36] have conducted the numerical study with the help of the finite difference method on steady heat and mass transfer phenomena along with laminar free convective MHD flow of water-based nano-fluid inside a trapezoidal cavity by incorporating various nanoparticles such as Ag, Cu, Al₂O₃, and TiO₂. The study reveals that both Nu_{avg} and Sh_{avg} enhance when Cu and Ag are used as nanoparticles. Saritha and Kumar [37] have numerically reported for a square geometry comprising of the steady and laminar double diffusive free convective flow of Cu-H₂O nano-fluid by using the SIMPLE algorithm of the finite volume technique. Manaa et al. [38] have worked on combined heat and mass transfer involving the buoyancy-induced convective flow of a micropolar H₂O-based nano-fluid within a cubical geometry by using the finite-volume technique. They have applied various nanoparticles like Ag, Cu, Al₂O₃, and TiO₂ from the analysis point of view. This work reveals that both Nu_{avg} and Sh_{avg} reduce with the augmentation of nanoparticle concentration. Al-Balushi et al. [39] have carried out a numerical examination with the support of a finite element approach for the thermo-solute and laminar free convective flow of magnetic nanofluid (base fluid: H₂O, engine-oil, and kerosene and magnetic nanoparticles: Fe₃O₄, SiO₂, Mn-ZnFe₂O₄, and CoFe₂O₄) inside a 3-D rectangular-shaped cuboid imposed to an inclined magnetic field. It is concluded that Mn-ZnFe₂O₄-kerosene nanofluid has the highest heat transfer characteristics (optimum Nu_{avg}) as compared to

the other nanofluid combinations. Umavathi et al. [40] have reported for the steady thermo-solute and laminar free convective flow of H₂O-based nanofluid inside a duct of rectangle shape by conducting numerical analysis with the help of the finite difference method. They have used several nanoparticles like Ag, Cu, SiO₂, Diamond, and TiO₂. It is observed that highest and minimum velocities are attained by the application of Ag and Diamond respectively. Also, maximum and minimum temperatures are established for SiO₂ and Diamond respectively. On the other hand, maximum and minimum concentrations are obtained with Diamond and SiO₂ respectively.

The positions of heating and cooling zones within the enclosure significantly affect thermo-solute transport phenomena. Further to that, few real-life applications of science and engineering (cooling of electronic systems, heat exchangers, medical and nuclear science, solar energy storage, chemical and processing industries etc.) ask for discrete and non-uniform heating. The discrete functions such as sinusoidal, exponential, etc. are adopted as the non-uniform source of heat under this scenario. In view of this, multiple authors have investigated for the convection heat and mass transfer mechanism within different cavities with their surfaces subjected to partial and non-uniform thermal arrangements. Past studies reveal that geometries subjected to sinusoidal heating conditions result into augmented thermal transport features as compared to the uniform heating case.

Uddin et al. [41] have numerically investigated with the aid of Galerkin's weighted residual iterative technique of finite-element method for the double-diffusion unsteady, laminar, and mixed convective flow in a lid-driven trapezoidal cavity subjected to uniform magnetic field along with uniform and non-uniform (sinusoidal manner) heat-mass source combination at the bottom surface. It is observed that heat and mass transfer rates for non-uniform heating and concentration case are smaller as compared to the uniformly heated and concentrated situation. Nath and Murugesan [42] have considered the flow of Cu-Al₂O₃-H₂O mixed nanofluid within a step channel having backward-facing subjected to an oriented magnetic field along with partial heating situations for the analysis of steady double-diffusion mixed and laminar convection phenomena in a numerical manner by utilizing the technique of finite-element. This study tells that heat and mass transport increase for $N > 0$. Gholizadeh et al. [43] have utilized the finite-difference technique for numerical investigation of the unsteady double-diffusive and natural convective laminar flow in

a trapezoidal domain having different orientations along with partial heating and concentration. Parvin et al. [44] have numerically worked with the aid of Galerkin's finite-element technique for $\text{Al}_2\text{O}_3\text{-H}_2\text{O}$ nanofluid flow inside a partially heated square cavity having double-diffusion steady and laminar free convection. This study talks about the major impact of Ra and nanoparticle concentration on the thermo-solute behavior inside the geometry taken. Nikbakhti and Rahimi [45] have numerically investigated by using the finite-difference methodology on the steady double diffusion and laminar free convection of air in a rectangular enclosure subjected to partial temperature-concentration effect. They have taken nine distinct thermal active regions for getting optimum transport conditions within the geometry. Mahapatra et al. [46] have mathematically examined by adopting the finite-difference technique for a transient double-diffusive and laminar mixed convective flow in a lid-driven square enclosure imposed to uniform as well as sinusoidal heating-concentration combination. Arani et al. [47] have conducted the numerical study with the aid of a finite-volume technique for the flow of $\text{Al}_2\text{O}_3\text{-H}_2\text{O}$ nano-fluid inside a partially heated and concentrated square geometry employing steady double-diffusive and laminar free convection. The study implies that both Nu_{avg} and Sh_{avg} enhance with the increment in Ra and positive value of N.

Ghaffarpassand [48] has numerically worked on MHD mixed convective flow of $\text{Cu-H}_2\text{O}$ nano-fluid along with combined heat and mass transfer within a square geometry subjected to partial uniform heat flux. Here, the finite-difference approach is used to solve the governing transport equations. He et al. [49] have conducted a numerical study on the thermo-solute free convective flow of $\text{Cu-H}_2\text{O}$ nanofluid within a square domain by using the lattice Boltzmann technique. Here, two vertical partitions having heat conduction are connected to the top and bottom surfaces of the cavity. This work reveals that the location of partitions plays a significant role towards the heat-species transport phenomena. Parveen and Mahapatra [50] have numerically reported for the thermo-solute magneto-hydrodynamic steady and free convective flow of $\text{Al}_2\text{O}_3\text{-H}_2\text{O}$ nano-fluid within a wavy configuration having entropy evolution. This investigation tells that both heat and mass transport enhance with the increment of Ra and nanoparticle concentration. Also, a rise in total entropy generation occurs with the increment of Ra. Afzalabadi et al. [51] have performed a numerical study by adopting the lattice Boltzmann technique for the steady double diffusion and laminar free MHD convective flow problem involving H_2O -based

nanofluids within a square geometry having internally placed thermo-solute source. They have used distinct nanoparticles such as Ag, Cu, and Al₂O₃ and pointed out that the most effective heat and species transfer are attained for Ag nanoparticles. Lu et al. [52] have numerically investigated with the assistance of the lattice Boltzmann technique for the thermo-solute buoyant-induced MHD convective phenomena inside a square enclosure having an internal heat conducting partition. It is concluded that heat and mass transfer tends to be optimum when magnetic field inclination is 90⁰. Parveen et al. [53] have performed numerical computation on the combined heat and mass transfer phenomena involving MHD free convective flow of Cu-H₂O based nanofluid together with entropy production within a peculiar oriented 2-D cavity of dome-shape with discrete heating and concentration. It is reported that thermo-solute transport and entropy evolution become lowest when the geometry inclination is 135⁰.

Porous media is having improved overall thermal conductivity implemented by the researchers in recent times as an alternative technique to enhance the heat transfer parameters. It comprises of solid matrix and pores occupied by one or more liquids. Applications of a permeable medium are widely noticed and studied by the investigators in natural processes, industrial operations, and distinct disciplines of science and engineering like transport of moisture and contaminants in the soil, swamp cooling, oceanography, geothermal systems, cooling of electronic chips and equipment, solidification, heat exchangers, solar collectors, porous insulation systems, porous bearing, drying, food processing and petrochemical industry, fuel cells, energy storage medium, dumping of nuclear waste materials, thermal and material science, hydrology, biology, the field of chemical engineering and many more.

As per literature, extensive studies were conducted during recent years by the research community for the dual diffusion convection mechanism through the porous media in distinct forms. In such context, Khan et al. [54] have numerically worked on steady double-diffusion and laminar free convection in a 2-D right trapezoidal porous cavity by using the finite-difference technique. The analysis reveals that both Nu_{avg} and Sh_{avg} enhance with the increase of corrected Ra and corrected buoyancy ratio. Moukalled and Darwish [55] have numerically conducted analysis for a rhombic annulus geometry of porous type having steady double diffusive and free convective laminar flow by using the Patankar's finite-volume technique. In this study, the working substances are air and H₂O. It was observed that convection phenomena are predominant with the rise of Darcy number and porosity. Mondal and Sibanda [56]

have carried out a numerical study on the transient double diffusive free convective flow within a square cavity involving porous media by utilizing the finite-difference technique. Chowdhury et al. [57] have carried out the numerical simulation with the aid of Galerkin's iterative approach of the finite-element for the flow of $\text{Al}_2\text{O}_3\text{-H}_2\text{O}$ nano-fluid within a porous cavity in triangle shape involving steady double-diffusive and laminar free convection. This work reveals that the heat and mass transport rises and reduces respectively by the increment of nanoparticle concentration. Hadidi and Bennacer [58] have numerically reported by using the finite-volume technique for the combined thermal and mass transport along with free convection phenomena within a 3-D cubical geometry involving porous medium and binary fluid in the form of two partial vertical layers. Stajanko et al. [59] have considered a cubic geometry involving a porous medium for analyzing the combined steady thermo-solute and free laminar convective phenomena numerically with the help of the boundary element approach. This work reports that heat and species transfer increase with the increment of the positive value of N . Transient double diffusion free convection around a cylindrical geometry inside a 2-D cavity having porous media is numerically estimated by Xu et al. [60] with the use of lattice Boltzmann technique. This work implies that both Nu_{avg} and Sh_{avg} increase with the rise of Darcy number when Le is kept constant. Li et al. [61] have used a general finite difference approach along with the Newton-Raphson technique for numerical investigation of the thermo-solute mechanism involving the steady and free convective flow of a porous medium within a parallelogram-shaped cavity subjected to differential heating-concentration effect.

Al-Farhany and Turan [62] have carried out numerical analysis with the aid of finite volume methodology along with the SIMPLER algorithm for the steady thermo-solute free convective mechanism inside an oriented porous cavity of square shape. It is found that Nu_{avg} and Sh_{avg} reduce and enhance respectively with the increment of Le for $N \leq -1$. Steady thermo-solute buoyant and MHD laminar convective flow of $\text{Al}_2\text{O}_3\text{-H}_2\text{O}$ nano-fluid saturated with porous media inside a trapezoidal geometry has been numerically investigated with the assistance of finite-difference technique by Saha et al. [63]. The outcome of this work is that heat and mass transfer rises and reduces respectively with the increment of nanoparticle concentration. Also, thermo-solute transport (Nu_{avg} and Sh_{avg}) enhances with the augmentation of geometry aspect ratio. Wang et al. [64] have numerically reported by using the lattice Boltzmann approach for the double-diffusive free convective phenomena involving $\text{Al}_2\text{O}_3\text{-H}_2\text{O}$

nano-fluid flow within a 2-D oriented square porous enclosure imposed to differential heating-concentration along with MHD effect. This work implies the significant effect of the increase of cavity orientation on heat and species transfer at a large value of the Darcy number. Habibi and Zahmatkesh [65] have used the finite volume code together with TDMA for the numerical investigation of combined heat and mass transfer problems by considering free as well as the mixed convective flow of salt-H₂O based nano-fluids within porous geometries. They have incorporated several nanoparticles such as Ag, Cu, CuO, Al₂O₃, CNT, Co, Fe₃O₄, TiO₂, MgO, and ZnO for the analysis purpose. The study concludes that thermo-solute phenomena become optimum when CuO-salt-H₂O is utilized as the nano-fluid for both free and mixed convection flow regimes. He et al. [66] have utilized the lattice Boltzmann technique for numerical analysis of the thermo-solute buoyant convection within a differentially heated-concentrated square cavity comprised of two distinct porous media. It is found that improvement in heat and species transfer occurs with the increment of N at a high value of porosity. Marzougui et al. [67] have numerically analyzed for the combined heat and mass transfer together with buoyant laminar convection and entropy evolution within a trapezoidal-shaped porous geometry involving a binary ideal gas mixture. It is concluded that net entropy generation enhanced with the increment of the positive value of N . Reddy et al. [68] have performed numerical simulation by adopting the Galerkin's iterative approach of finite element for unsteady heat and species transfer involving laminar free convective cross flow inside an oriented trapezoidal-shaped porous cavity subjected to the differential temperature-concentration effect. Magnetic field impact on steady thermo-solute free convective flow together with entropy formation within a 2-D square enclosure having a porous circular cylinder located at the center has been numerically examined with the application of the lattice Boltzmann technique by Vijaybabu [69]. This work reveals that entropy evolution rises remarkably with the increment of buoyancy ratio, Darcy number, and magnetic field inclination.

Definite industrial operations deal with fluids possessing non-Newtonian characteristics. Newtonian fluids do not obey Newton's law of viscosity. Bingham plastic, Pseudo-plastic and dilatant fluids are a very popular class of non-Newtonian fluids. Examples of these fluids are fruit juice, ketchup, starch solutions, toothpaste, soap solution, shampoo, lubricants, blood, saliva, colloidal suspensions, lava, glues, paints, polymers (molten state), and so on. These fluids are imposed to combined heat

and species transfer through free convection mode while their synthesis. Past studies conclude that very less literature is available on non-Newtonian fluid flow, and it is very difficult to numerically estimate the behavior of such fluids.

In this connection, Tizakast et al. [70] have conducted the numerical analysis with the aid of the finite volume method for the double-diffusion mixed and laminar regime of convection inside a rectangular enclosure containing non-Newtonian fluid. In this work, the upper and bottom walls of the geometry are adiabatic and impermeable moving with the same uniform velocity in opposite directions. However, the vertical walls are given constant mass and heat flux. Kefayati [71] has worked on Bingham fluid ($Pr = 1$) flow within a 2-D inclined differentially heated and concentrated square enclosure involving laminar and free convective heat-mass transport phenomena along with entropy evolution by using the finite-difference lattice Boltzmann method. The investigation reveals that reduction in heat and mass transfer happens with the increase of Bingham number. Also, this study tells that reduction in net entropy generation is noticed for the increment of Bingham number and Eckert number. The combined heat and species transport process involving 2-D steady and laminar free convective flow of viscoplastic fluid as the working medium within a porous square enclosure has been numerically analyzed with the aid of the Lattice Boltzmann technique by the Kefayati [72]. This investigation reveals that when Darcy number is varied from 10^{-2} to 10^{-6} then heat-mass transport decreases. Hussain et al. [73] have utilized Galerkin's technique of finite-element for numerical computation of thermo-solute MHD and steady laminar free convective flow of Casson fluid together with the entropy evolution within a 2-D staggered porous enclosure. It is observed that both Nu_{avg} and Sh_{avg} enhance for the rise of Casson parameter. Additionally, net entropy generation reduces with the increase of Ha and Le .

Makayssi et al. [74] have conducted a numerical study with the aid of the finite difference method on combined heat and mass transfer phenomena involving laminar free convective flow of Carreau shear-thinning non-Newtonian fluid medium within a square-shaped enclosure. Nag and Molla [75] have numerically worked on the thermo-solute free convective Al_2O_3 - H_2O -based nano-fluid flow inside a 2-D square enclosure imposed to differential temperature-concentration effect for analyzing the non-Newtonian impact by utilizing the finite volume code. In this work, the non-Newtonian response of the fluid is illustrated with the application of the

viscosity model of the power law. It is observed that both heat transfer (Nu_{avg}) and species transport (Sh_{avg}) reduce with the increment of the power-law exponent. Kolsi et al. [76] have used the Galerkin's iterative approach of finite-element for numerical investigation of the steady dual diffusion buoyancy-induced laminar convection phenomena inside a square geometry comprising working substance as a porous medium and non-Newtonian fluid layer distinguished through a sinusoidal interface. It is observed that both Nu_{avg} and Sh_{avg} reduce with the increment of the power law exponent.

Liquid metals consist of low melting point alloys. They are in the liquid phase at room temperature conditions, and this leads to their wider use as a cooling agent in several engineering applications like nuclear reactors, metal processing and so on. In such context, Sathiyamoorthi and Anbalagan [77] have conducted a numerical study by using the lattice Boltzmann technique on combined heat and mass transfer along with steady laminar buoyant MHD convective flow of NaK as liquid metal ($Pr = 0.054$) and entropy generation within a square geometry involving an insulated block of rectangular shape placed at the very middle. The study reveals that total entropy evolution enhances with the increment of Ra and Le . However, it reduces with the increase of Ha . Further to that, Sathiyamoorthi et al. [78] have performed a numerical investigation by adopting the lattice Boltzmann method on the steady double diffusion and laminar buoyancy-induced MHD convective flow of liquid metal inside a 2-D square enclosure incorporating an adiabatic block of rectangle shape positioned at the very center. In this study, the various operating parameters are $Ra (= 10^3 - 10^5)$, $Le (= 2 - 10)$, $N (= -2 \text{ to } 2)$, and $Ha (= 0 - 50)$.

1.3 Inspiration and Purpose behind the Work

Evidently, the above literature survey reveals that dual diffusive laminar mixed convective flow of water within a square cavity subjected to differential heating from left to right and differential concentration from top to bottom in the absence and presence of magnetic effect has not been numerically investigated till date. Therefore, this inspires us to perform further computational analysis on the double diffusion hybrid convection mechanism having newly flow configuration to cover such a study gap in the research domain and this also asserts the novelty of the current work.

The main purpose of this work is to conduct numerical simulation on combined heat and mass transfer convective phenomena of H₂O inside a lid-driven square enclosure with differential temperature-concentration boundary conditions by adopting two situations: a) without a magnetic field and b) with a magnetic field. Here, the Finite Element Method based solver is used to numerically solve the problem in hand and the results are interpreted in terms of the various non-dimensional parameters namely Reynolds number (Re), Richardson number (Ri), Lewis number (Le), Buoyancy ratio (N), and Hartmann number (Ha). The effects of variation of these parameters are reported on Streamline contours, Isotherm plots, Iso-concentration curves, Heatlines, global heat (Nu_{avg}) and mass transfer (Sh_{avg}) characteristics to explore the thermo-fluidic behavior along with the species flow within the geometry taken.

1.4 Structure of the Work

At the very beginning of Chapter 1, the introduction section incorporates the fundamentals of the double diffusion convection process along with their practical significance and utilities. Further to that, the associated literature review is extensively provided and after that aim of the study along with its novelty is covered. In continuation of this, Chapter 2 includes the mathematical modeling and numerical technique associated with the problem, which is appropriately covered in sub-sections 2.1, 2.2, and 2.3. Then, Chapter 3 comprises of simulation results along with their discussion as described in sections 3.1, 3.2, 3.3, 3.4, 3.5, and 3.6. Finally, the scope of future extension of the present work is mentioned in Chapter 4. The list of pertinent citations utilized to perform this numerical verification is provided at the end of Chapter 4.

CHAPTER – 2

Mathematical Modelling and Numerical Technique

2.1 Physical Description of the Problem

Here, Fig. 2.1 (a) represents a model of the problem adopted with the computing domain as a 2-D square cavity ($A = 1$) having width W and height H , incorporating H_2O ($Pr = 5.83$) as the working medium. It is quite clear that the left-hot wall and right-cold wall of the cavity is kept at uniform temperatures of T_h and T_c respectively and they are impermeable as well, causing no mass transfer through them. Further to that the top and bottom walls are insulated, ensuring no heat transfer through them and they are subjected to high concentration (c_h) and low concentration (c_c). Also, the upper wall surface is imposed to rightward motion with velocity U_0 which results in the lid-driven enclosure. Gravity (g) works in a vertically downward direction. It is important to mention here that buoyant forces are developed because of differential heating-concentration conditions provided to the walls and these forces are employed with the assistance of Boussinesq's approximation. Therefore, the referred problem can be defined as the double diffusion mixed convection one; where forced convection effects are accounted for due to lid-driven geometry configuration and buoyant forces establishing free convective flow.

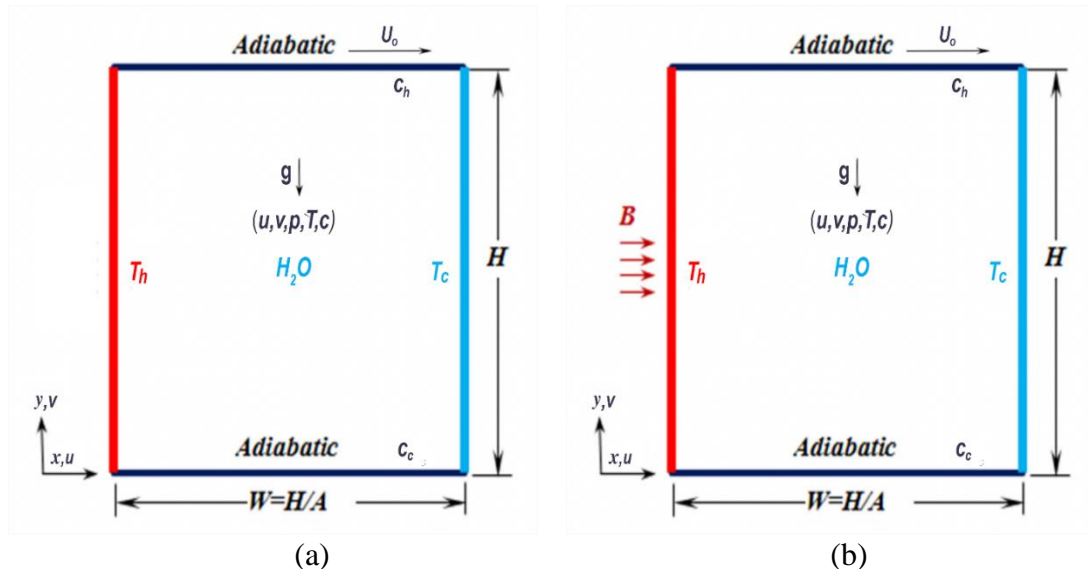


Fig. 2.1: Schematic Diagram for the Considered Problem Geometry (a) Absence of the Magnetic Field and (b) Presence of the Magnetic Field.

In continuation of the above, Fig. 2.1 (b) shows the very similar type of problem. Only the change is that a total and uniform magnetic field represented by the

notation B ; is applied to the computational domain in a horizontal direction to study the magneto-hydrodynamic effects associated with the double-diffusive mixed convective phenomena. Here, the magnetic field produces the magnetic force namely Lorentz force which opposes the existing buoyant forces within the enclosure. The intensity of such magnetic force is controlled by changing the value of Ha and which is further utilized to govern the thermo-solute flow mechanism.

It is supposed that the fluid is Newtonian and incompressible. In the momentum equation, body forces are considered by using the Boussinesq approximation indicated by equation (1).

$$\rho = \rho_0[1 - \beta_T(T - T_c) - \beta_S(c - c_c)] \quad (1)$$

For the current problem, the governing transport equations are formulated, and they are given by the 2-D steady continuity, momentum, energy, and concentration equations as follows:

$$\frac{\partial u}{\partial x} + \frac{\partial v}{\partial y} = 0 \quad (2)$$

$$\left(u \frac{\partial u}{\partial x} + v \frac{\partial u}{\partial y}\right) = -\frac{1}{\rho} \frac{\partial p}{\partial x} + \nu \left(\frac{\partial^2 u}{\partial x^2} + \frac{\partial^2 u}{\partial y^2}\right) \quad (3)$$

$$\left(u \frac{\partial v}{\partial x} + v \frac{\partial v}{\partial y}\right) = -\frac{1}{\rho} \frac{\partial p}{\partial y} + \nu \left(\frac{\partial^2 v}{\partial x^2} + \frac{\partial^2 v}{\partial y^2}\right) + g[\beta_T(T - T_c) - \beta_S(c - c_c)] \quad (4)$$

$$\left(u \frac{\partial T}{\partial x} + v \frac{\partial T}{\partial y}\right) = \alpha \left(\frac{\partial^2 T}{\partial x^2} + \frac{\partial^2 T}{\partial y^2}\right) \quad (5)$$

$$\left(u \frac{\partial c}{\partial x} + v \frac{\partial c}{\partial y}\right) = D \left(\frac{\partial^2 c}{\partial x^2} + \frac{\partial^2 c}{\partial y^2}\right) \quad (6)$$

The above dimensional form of governing equations can be reduced to non-dimensional form with the help of some suitable scaling factors as given below:

$$X = \frac{x}{W}, Y = \frac{y}{W}, U = \frac{u}{U_0}, V = \frac{v}{U_0}, P = \frac{p}{\rho U_0^2}, \theta = \frac{T - T_c}{T_h - T_c}, C = \frac{c - c_c}{c_h - c_c} \quad (7)$$

The dimensionless equations are expressed as

$$\frac{\partial U}{\partial X} + \frac{\partial V}{\partial Y} = 0 \quad (8)$$

$$\left(U \frac{\partial U}{\partial X} + V \frac{\partial U}{\partial Y}\right) = -\frac{\partial P}{\partial X} + \frac{1}{Re} \left(\frac{\partial^2 U}{\partial X^2} + \frac{\partial^2 U}{\partial Y^2}\right) \quad (9)$$

$$\left(U \frac{\partial V}{\partial X} + V \frac{\partial V}{\partial Y}\right) = -\frac{\partial P}{\partial Y} + \frac{1}{Re} \left(\frac{\partial^2 V}{\partial X^2} + \frac{\partial^2 V}{\partial Y^2}\right) + Ri(\theta + NC) \quad (10)$$

$$\left(U \frac{\partial \theta}{\partial X} + V \frac{\partial \theta}{\partial Y}\right) = \frac{1}{Re Pr} \left(\frac{\partial^2 \theta}{\partial X^2} + \frac{\partial^2 \theta}{\partial Y^2}\right) \quad (11)$$

$$\left(U \frac{\partial C}{\partial X} + V \frac{\partial C}{\partial Y}\right) = \frac{1}{Le Re Pr} \left(\frac{\partial^2 C}{\partial X^2} + \frac{\partial^2 C}{\partial Y^2}\right) \quad (12)$$

The pertinent boundary conditions are as follows:

Velocity: $U = V = 0$ at $X = 0, X = 1, Y = 0$ and $V = 0, U = 1$ at $Y = 1$.

Temperature: $\theta = 1$ at $X = 0$, $\theta = 0$ at $X = 1$ and

$$\frac{\partial \theta}{\partial Y} = 0 \text{ at } Y = 0, Y = 1 \quad (13)$$

Concentration: $C = 1$ at $Y = 1$, $C = 0$ at $Y = 0$ and $\frac{\partial C}{\partial X} = 0$ at $X = 0, X = 1$

Again, the global parameters such as average Nusselt number and average Sherwood number can be estimated by using the following formulas:

$$Nu_{avg} = \int_0^1 \left(-\frac{\partial \theta}{\partial X} \right)_{X=0} dY \text{ and } Sh_{avg} = \int_0^1 \left(-\frac{\partial C}{\partial Y} \right)_{Y=0} dX \quad (14)$$

2.2 Numerical Technique

Here, Galerkin's weighted residual iterative approach of finite elements is employed to solve the problem by considering an appropriate grid size. The technique is used to discretize the non-dimensional governing transport equations and subsequently, solution results are generated. The results are presented through contour plots like streamlines, isotherms, iso-concentration, heat lines and global parameters (Nu_{avg} and Sh_{avg}). The detailed working procedure of FEM is represented by the block diagram as shown in Fig. 2.2.

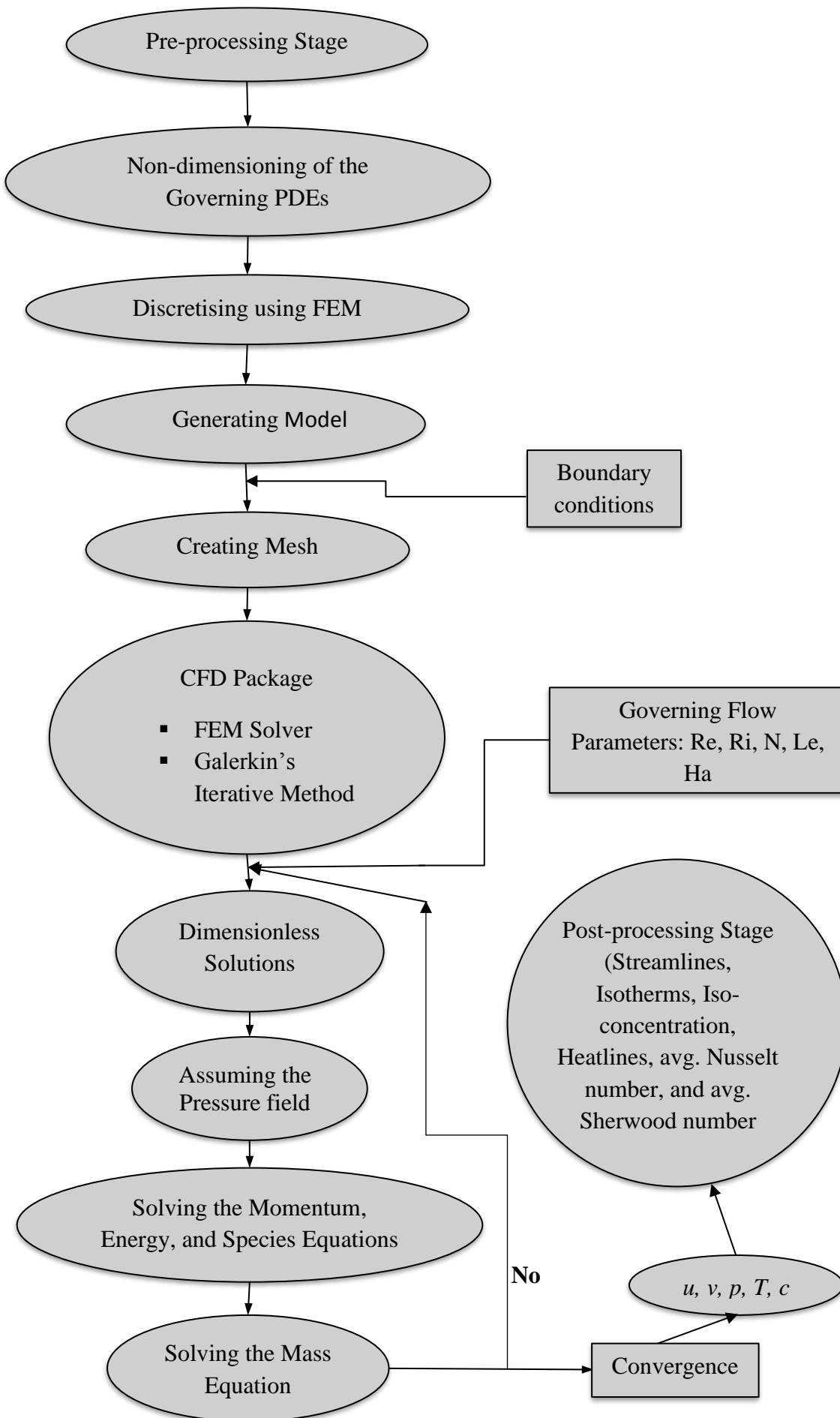


Fig. 2.2: Block Diagram Representation of the Solution Technique using FEM

2.3 Validation Study

The previous published numerical work of Al-Amiri et al. [1] is considered here for the validation of the present FEM code. In such context, Fig. 2.3 represents the variation of the average Nusselt number with N ($= -100$ to 100) for two different values of Ri viz. 0.01 and 1 by keeping $Re = 100$ and $Le = 1$ as a fixed value. It is obvious that the results of the present work are in good agreement with the past referred work of Al-Amiri and hence this justifies the validity of the solver. Ultimately, the solver can be frequently adopted for the extensive simulation works leading to good accuracy.

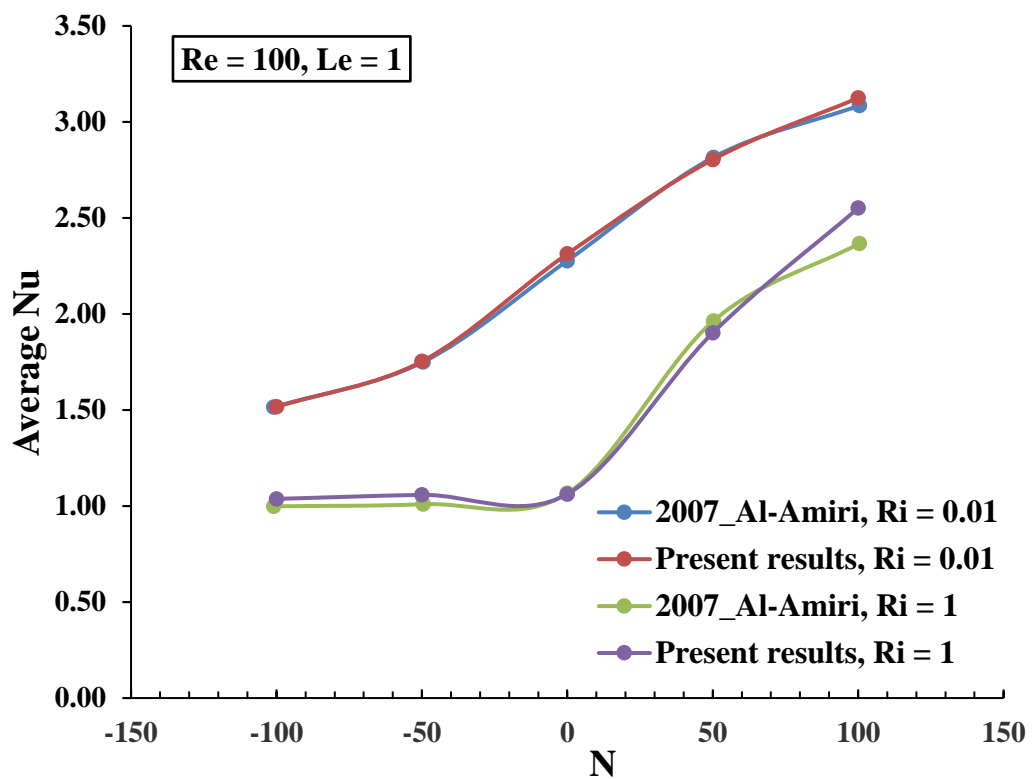


Fig. 2.3: Comparison of the present FEM code with the Al-Amiri [1] work.

CHAPTER – 3

Results and Discussion

In the present chapter, the impacts of the change of distinct flow governing variables along with their broad range like Re ($= 10 - 100$), Ri ($= 0.1 - 10$), Le ($= 1 - 5$), N ($= -10 - 10$), Ha ($= 0 - 80$) at $Pr = 5.83$ are highlighted for the chosen computational domains involving the steady double-diffusive mixed convective laminar flow of H_2O together with imposed boundary conditions. The effects of these controlling parameters are presented and discussed using the contours of streamline, isotherm, iso-concentration, heat line and overall thermo-solute features represented by average Nusselt (Nu) and average Sherwood (Sh) numbers, respectively.

3.1 Effect of Variation of Ri and Re

Fig. 3.1 represents variation of streamlines for various values of Ri ($= 0.1, 1, 10$) and distinct magnitudes of Re ($= 10, 50, 100$) at fixed values of $N = 1$, $Le = 1$, and $Ha = 0$. It is noted that clockwise circulation is established within the cavity throughout the study range. At $Ri = 0.1$ for all values of Re , the flow pattern is almost identical having an increased density of streamlines in the middle of the cavity. However, for $Ri = 1$ at $Re = 50$ and $Re = 100$ the vortices slightly shift towards the upper right corner as compared to the $Re = 10$ cases. Again, it is observed that for $Re = 50$ at $Ri = 10$ significant change occurs in the flow structure as compared to the $Re = 10$ situation: with irregular and distorted vortex shape along with the appearance of additional vortex formation near the bottom left corner. On the contrary, with a high value of $Re = 100$ at $Ri = 10$ the additional vortex separates out from the main vortices with expansion in the right direction. This is because, at a high value of Re , the velocity of flow would be more leading to the enhancement in the transport phenomena.

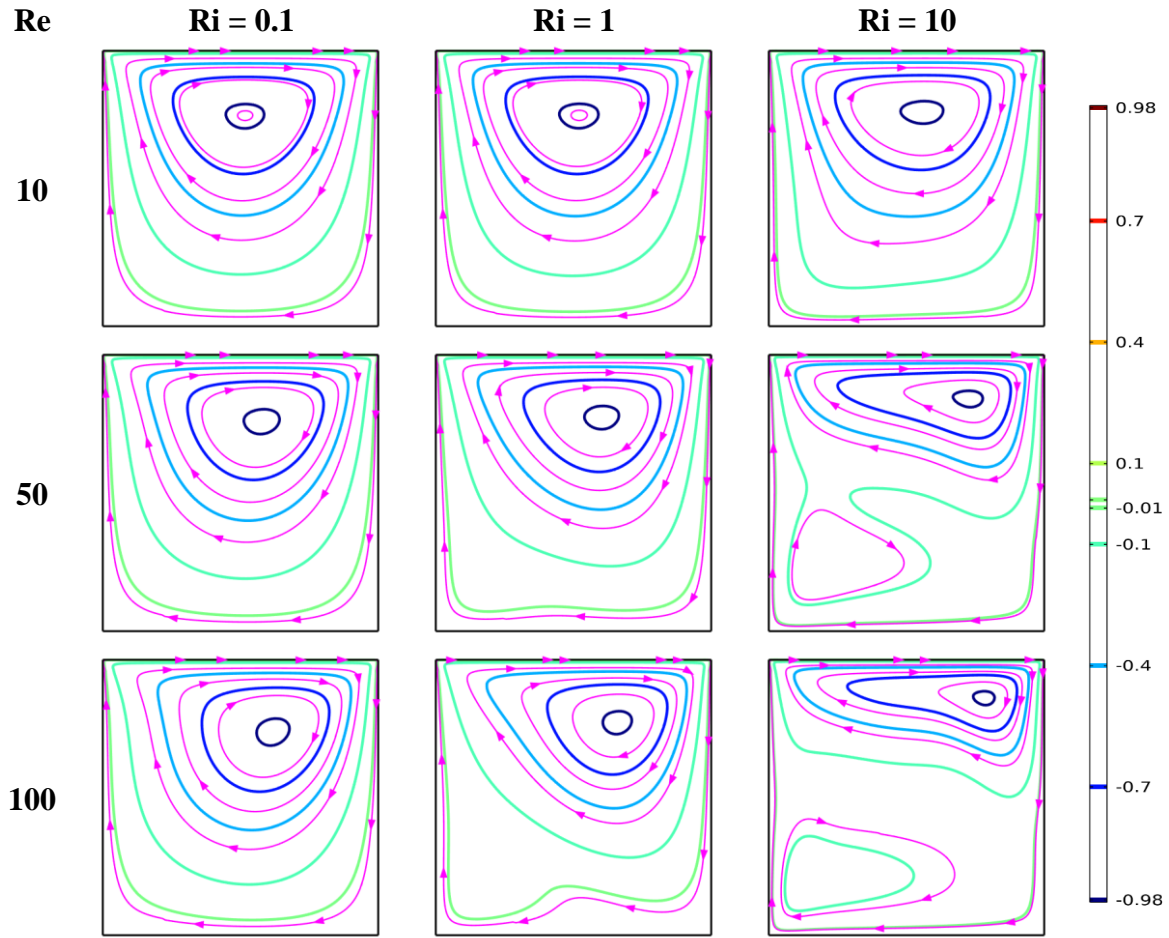


Fig. 3.1: Streamline Contours for $N = 1$, $Le = 1$ at $Ha = 0$.

The distribution of the isotherms for distinct values of Ri ($= 0.1, 1, 10$) and various values of Re ($= 10, 50, 100$) by keeping $N = 1$, $Le = 1$, and $Ha = 0$ as fixed parameters is represented through the figure Fig. 3.2. At $Re = 10$ for all values of Ri , the temperature distribution is very much similar. Near the left wall, it is entirely vertical but shows some orientation at the middle of the cavity. However, at $Re = 50$ significant change is noticed in temperature behavior, especially at $Ri = 10$ case, where the temperature profile reflects the wavy pattern in the vicinity of the left hot wall and non-linear feature throughout the cavity. Further to that for $Re = 100$ at $Ri = 10$, the non-linear isotherms shift towards rightward. As at a high Re value increase in velocity leads to subsequent enhancement in heat transfer where forced convection effects would dominate over the natural one.

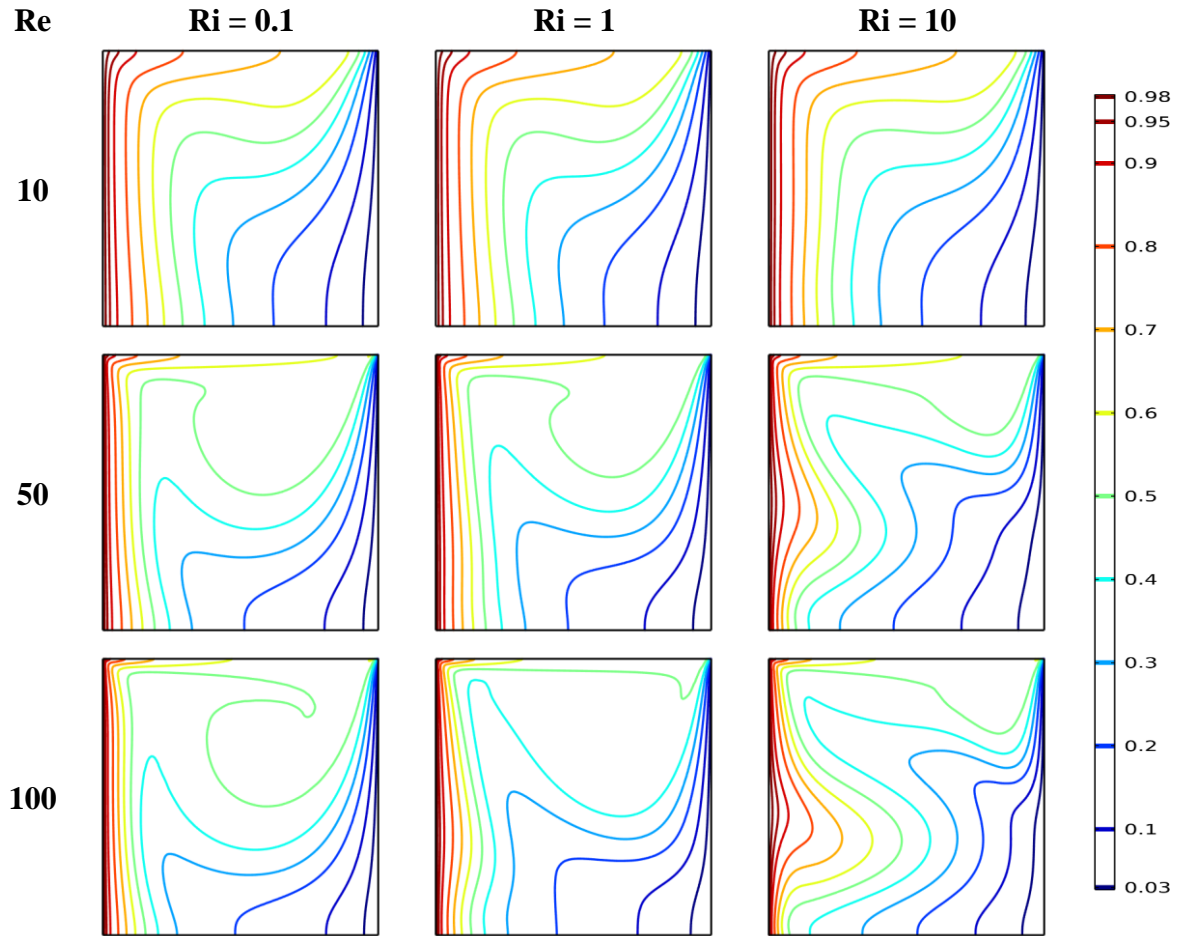


Fig. 3.2: Isotherm Plots for $N = 1$, $Le = 1$ at $Ha = 0$.

Fig. 3.3 represents variation of iso-concentration contours for various values of Ri ($= 0.1, 1, 10$) and distinct magnitudes of Re ($= 10, 50, 100$) at fixed values of $N = 1$, $Le = 1$, and $Ha = 0$. At $Re = 10$ for all values of Ri the mass contours are almost identical with flat lines at the bottom and orientated towards the top right corner. Now with all values of Ri for both $Re = 50$ and $Re = 100$, a major change in mass transfer behavior is observed. This is because thinner concentration boundary layers are produced near the low concentrated bottom wall. Also, the flow velocity is increased at high magnitude of Re leading to subsequent enhancement in species transfer rate.

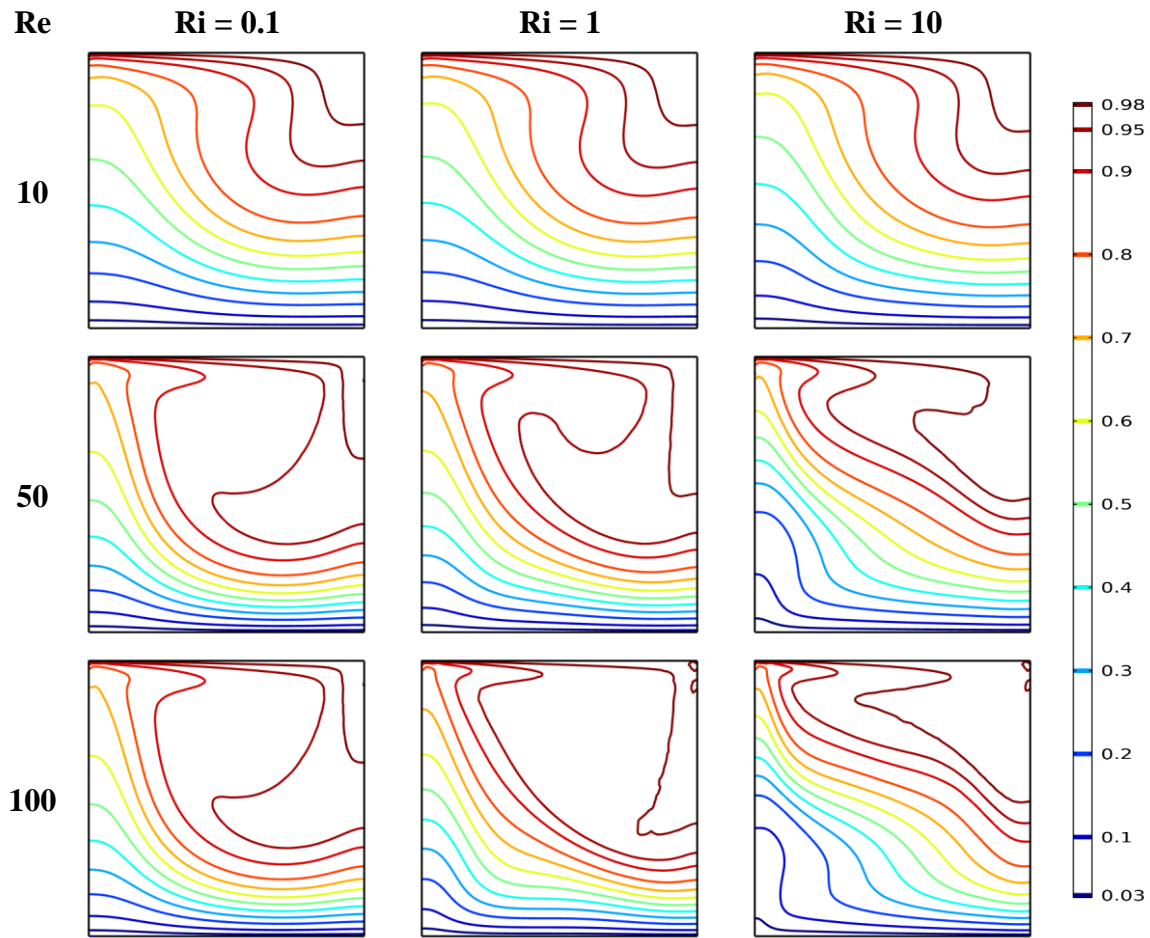


Fig. 3.3: Concentration Curves for $N = 1$, $Le = 1$ at $Ha = 0$.

The distribution of the heat lines for distinct values of Ri ($= 0.1, 1, 10$) and various values of Re ($= 10, 50, 100$) by keeping $N = 1$, $Le = 1$, and $Ha = 0$ as fixed parameters is represented through the figure Fig. 3.4. It is observed that with both $Ri = 0.1$ and $Ri = 1$ at $Re = 10$ the distribution of thermal energy is similar. However, for $Ri = 10$ at $Re = 10$ heat lines slightly shift towards the left wall. In such a situation at a high value of Ri , the transport of thermal energy happens through free convection mode. When Re is further increased up to 50 and 100 then heat lines reflect the notable change for all values of Ri ; especially at $Ri = 10$. Since at a high value of Re , transport of heat energy takes place in the rightward direction through the forced convection regime.

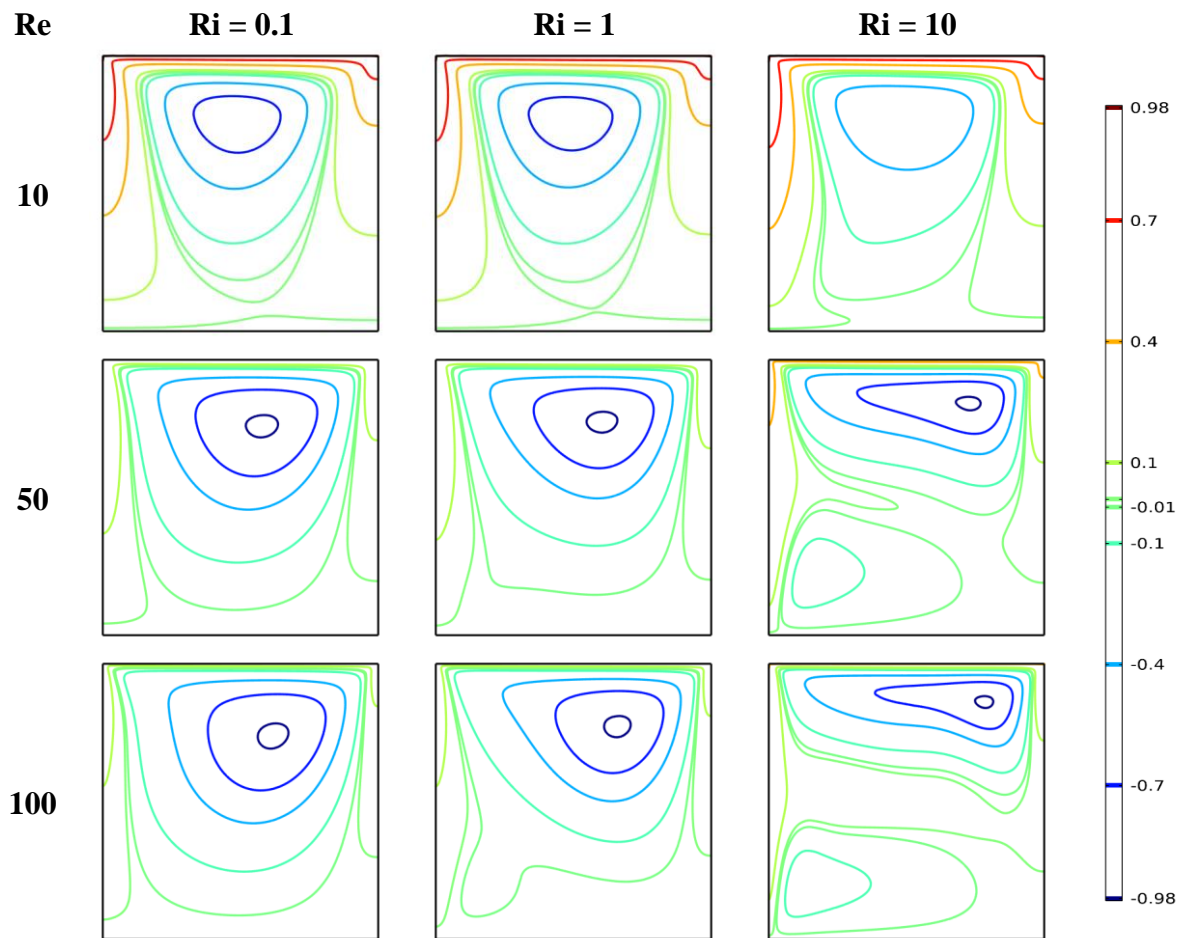


Fig. 3.4: Heat lines for $N = 1$, $Le = 1$ at $Ha = 0$.

3.2 Effect of Variation of Ri and Le

Fig. 3.5 represents variation of the streamlines for various values of Ri ($= 0.1, 1, 10$) and distinct magnitudes of Le ($= 1, 3, 5$) at fixed values of $Re = 50$, $N = 1$, and $Ha = 0$. It is noted that clockwise circulation is established within the geometry throughout the study range. For all values of Le at $Ri = 0.1$, streamline contours are almost identical. When Ri is increased up to 1 then the flow structure slightly shifts towards the right direction. On the other hand, flow structure reflects irregular and distorted vortex shape along with the appearance of additional vortex formation near the bottom left corner for $Ri = 10$ at $Le = 1$. Further to that for $Ri = 10$ at $Le = 3$ and $Le = 5$ the additional vortex separates out from the main vortices.

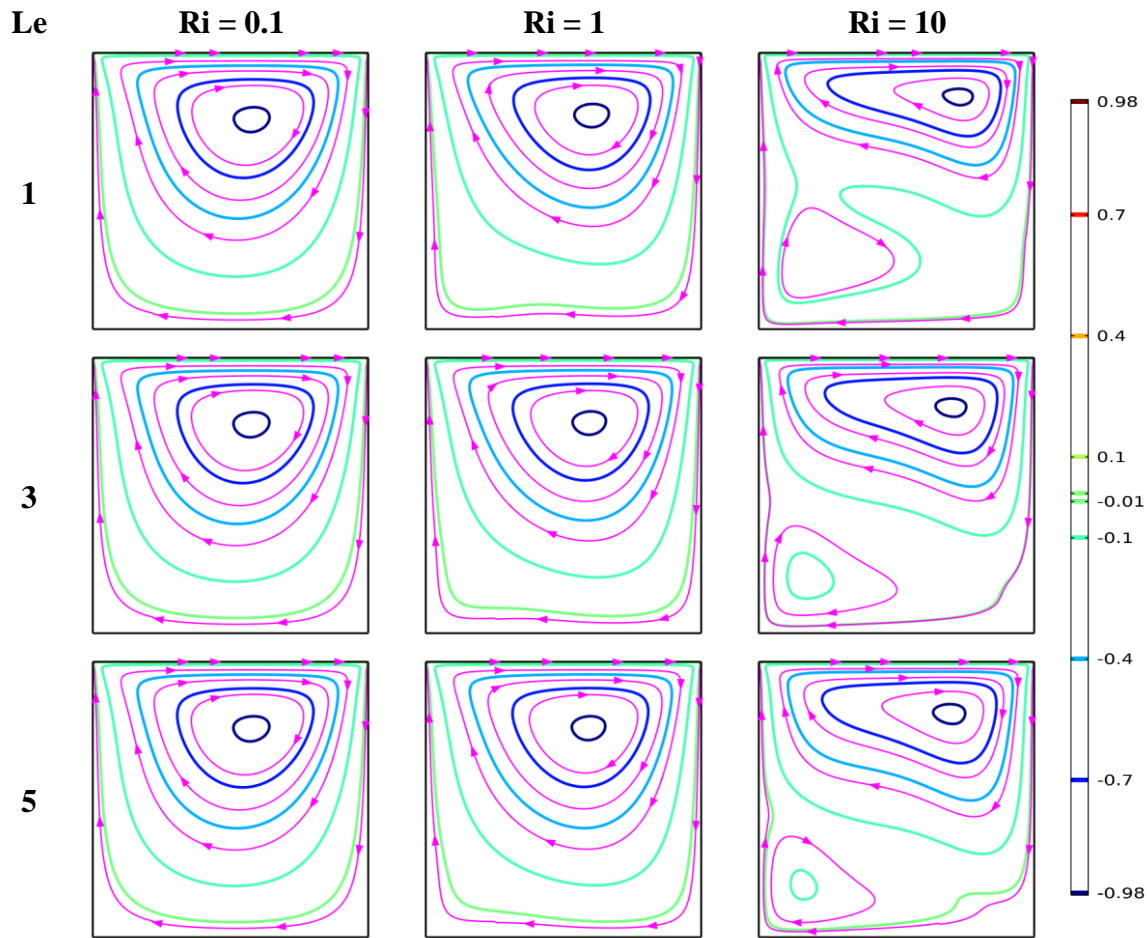


Fig. 3.5: Streamline Contours for $Re = 50$, $N = 1$ at $Ha = 0$.

The distribution of the isotherms for distinct values of Ri ($= 0.1, 1, 10$) and various values of Le ($= 1, 3, 5$) by keeping $Re = 50$, $N = 1$, and $Ha = 0$ as fixed parameters is represented through the figure Fig. 3.6. It is quite clear that temperature distribution is almost identical for both $Ri = 0.1$ and $Ri = 1$ for all values of Le . On the contrary, when Ri is increased up to 10 then significant change is recognized in isotherms such that the temperature profile reflects the wavy pattern in the vicinity of the left hot wall. However, they are very similar for all values of Le . It is important to note here that the free convective mode of heat transfer is governing one at a high value of Ri and at a high value of Le thermal diffusive effect would pre-dominate over the mass diffusivity.

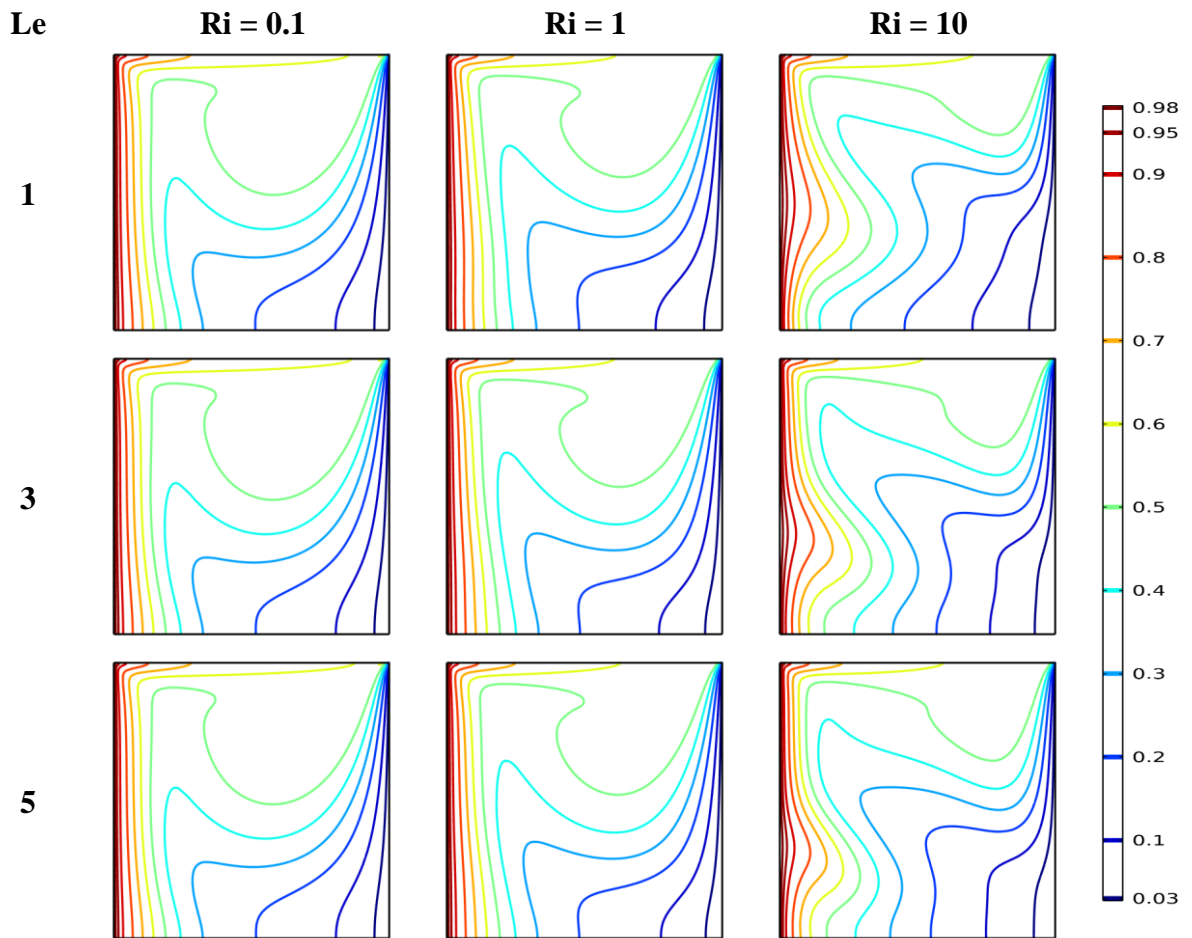


Fig. 3.6: Isotherm Plots for $Re = 50$, $N = 1$ at $Ha = 0$.

Fig. 3.7 represents variation of the mass contours for various values of Ri ($= 0.1, 1, 10$) and distinct magnitudes of Le ($= 1, 3, 5$) at fixed values of $Re = 50$, $N = 1$, and $Ha = 0$. It is observed that the mass transfer pattern varies for all values of Ri at $Le = 1$. However, these lines are almost identical for both $Le = 3$ and $Le = 5$ for various values of Ri . As at the high value of Le , the thermal boundary layer would be thicker than the concentration boundary layer. This ensures the enhancement in species transfer which is going to take place from the top wall to the bottom wall of the geometry.

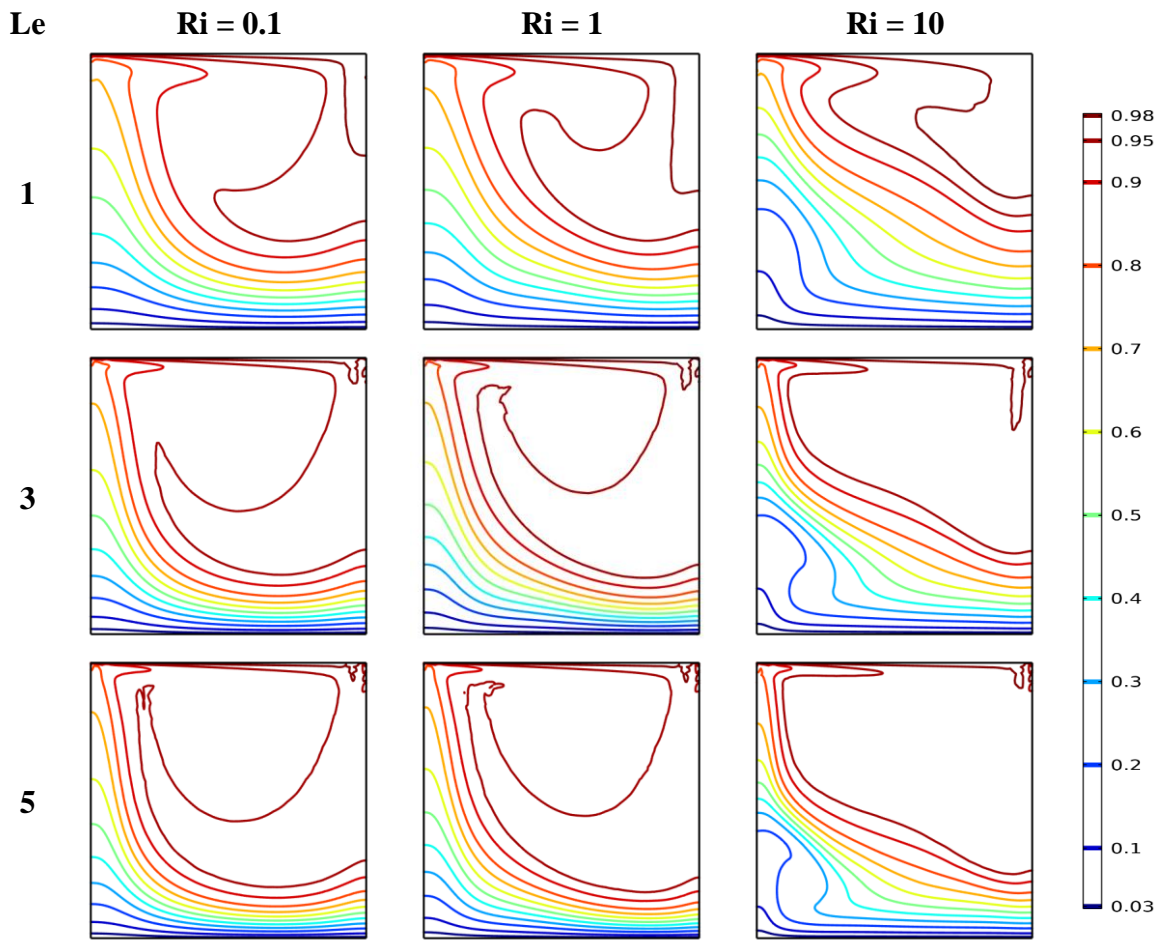


Fig. 3.7: Concentration Curves for $Re = 50$, $N = 1$ at $Ha = 0$.

The distribution of the heat lines for distinct values of Ri ($= 0.1, 1, 10$) and various values of Le ($= 1, 3, 5$) by keeping $Re = 50$, $N = 1$, and $Ha = 0$ as fixed parameters is represented through the figure Fig. 3.8. It is quite clear that thermal energy distribution is almost identical in the case of both $Ri = 0.1$ and $Ri = 1$ for all values of Le . On the contrary, when Ri is raised up to 10 for all values of Le then a major change in the pattern of heat transfer is observed. At high Ri , transport of the thermal energy is governed by the free convection regime of heat transfer from the left to the right wall in the cavity.

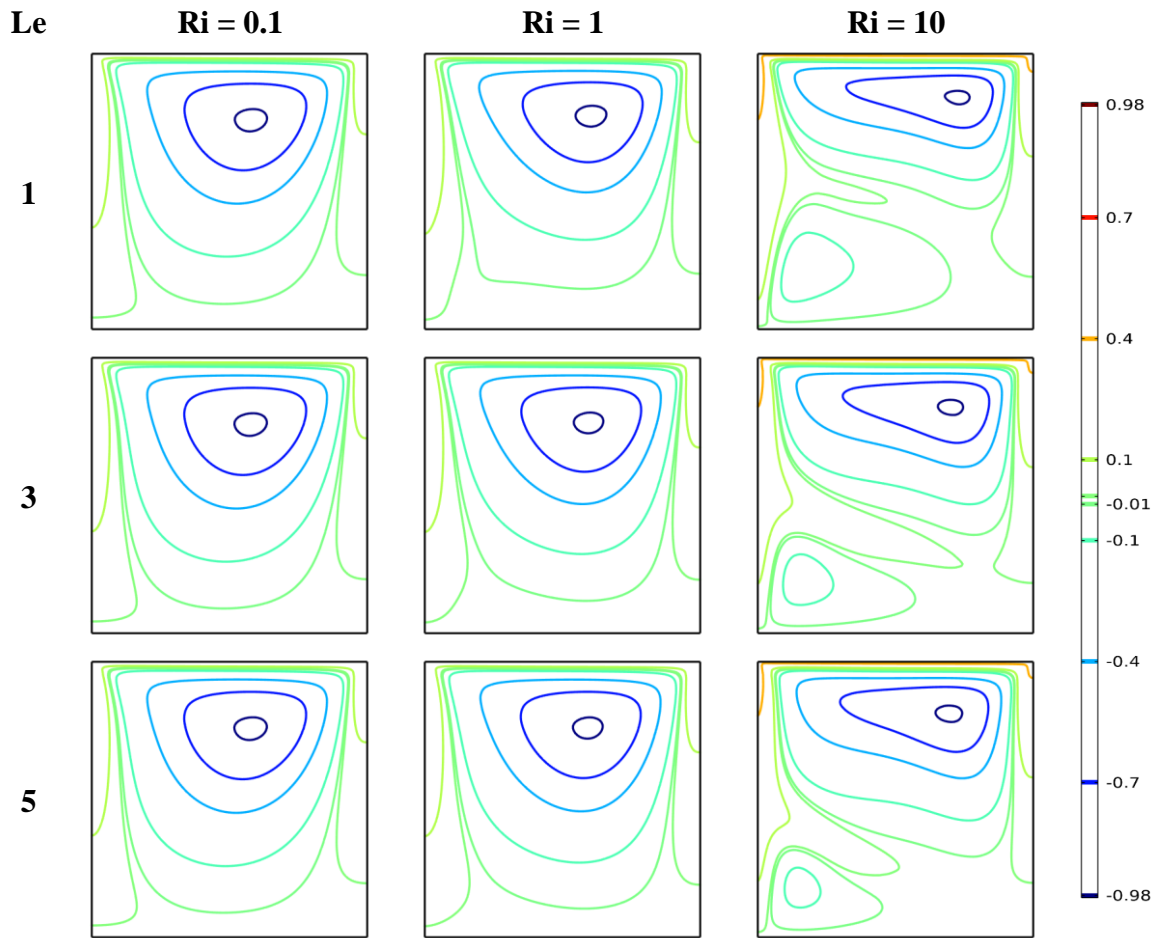


Fig. 3.8: Heat lines for $Re = 50$, $N = 1$ at $Ha = 0$.

3.3 Effect of Variation of Ri and N

Fig. 3.9 represents variation of the streamline for various values of Ri ($= 0.1, 1, 10$) and distinct magnitudes of N ($= -10$ to 10) at fixed values of $Re = 10$, $Le = 1$, and $Ha = 0$. When N is increased from -10 to 1 for both values of $Ri = 0.1$ and $Ri = 1$ then there is no significant change noticed in the flow structure. However, it changes for the increment of N from -10 to 1 at the higher magnitude of $Ri = 10$. Further to this, for both $Ri = 0.1$ and $Ri = 1$ at $N = 10$ additional vortices appeared in the geometry. In such connection, it is important to note that solute buoyancy force counteracts thermal buoyancy force at a negative value of N . At $N = 0$, only thermal buoyancy force exists. However, they become equal at $N = 1$. Also, for a positive high value of N solute buoyancy force dominate over the thermal one.

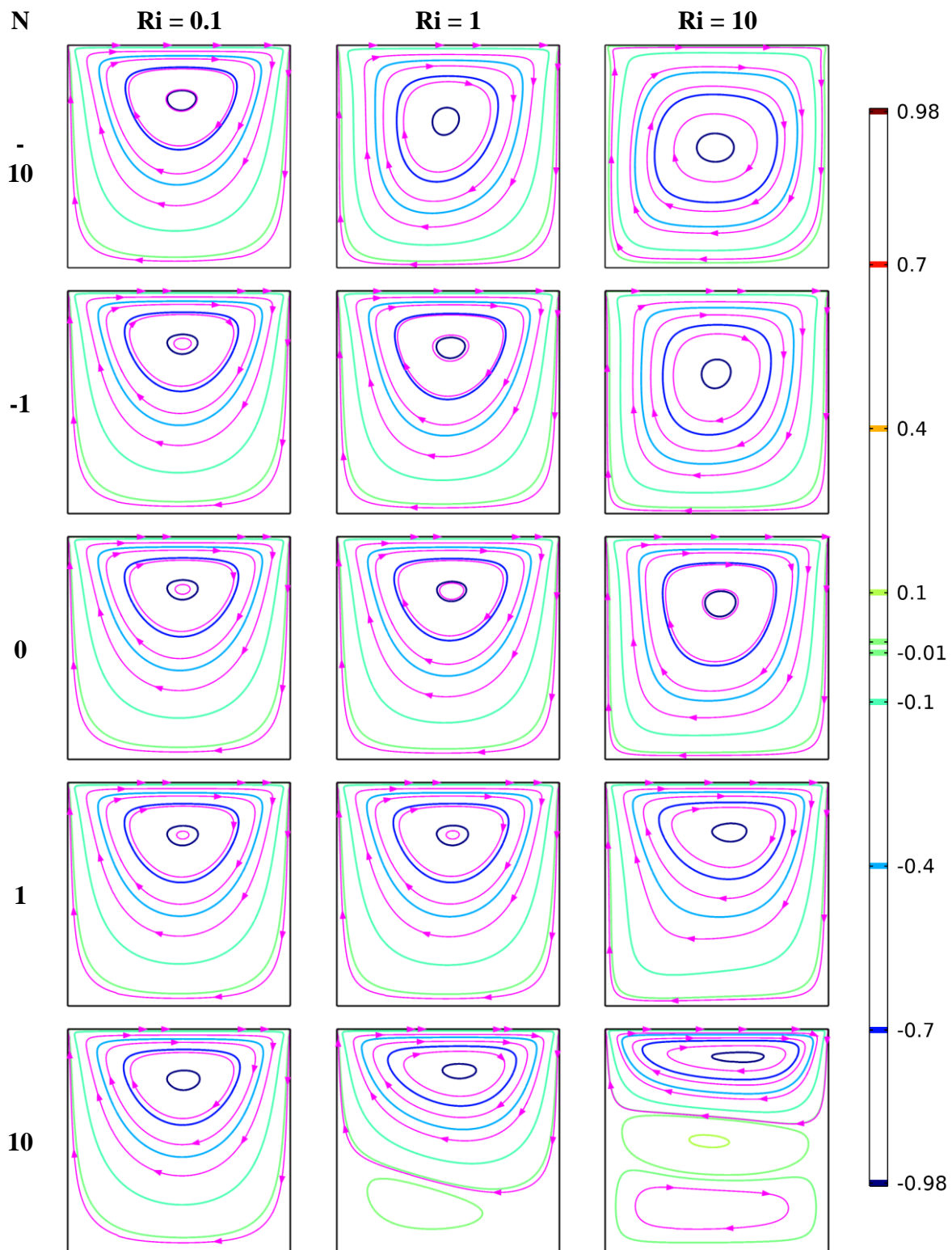


Fig. 3.9: Streamline Contours for $Re = 10$, $Le = 1$ at $Ha = 0$.

The distribution of isotherms for distinct values of Ri ($= 0.1, 1, 10$) and various magnitudes of N ($= -10$ to 10) at fixed values of $Re = 10$, $Le = 1$, and $Ha = 0$ is shown by Fig. 3.10. Here, temperature behavior remains almost the same for all values of N along with various Ri values except for $N = -10$ and $Ri = 10$. This is because, at a higher value of Ri , free convection governs the associated heat transfer phenomena. Also, at a negative higher value of N solute buoyancy force opposes the thermal buoyancy force.

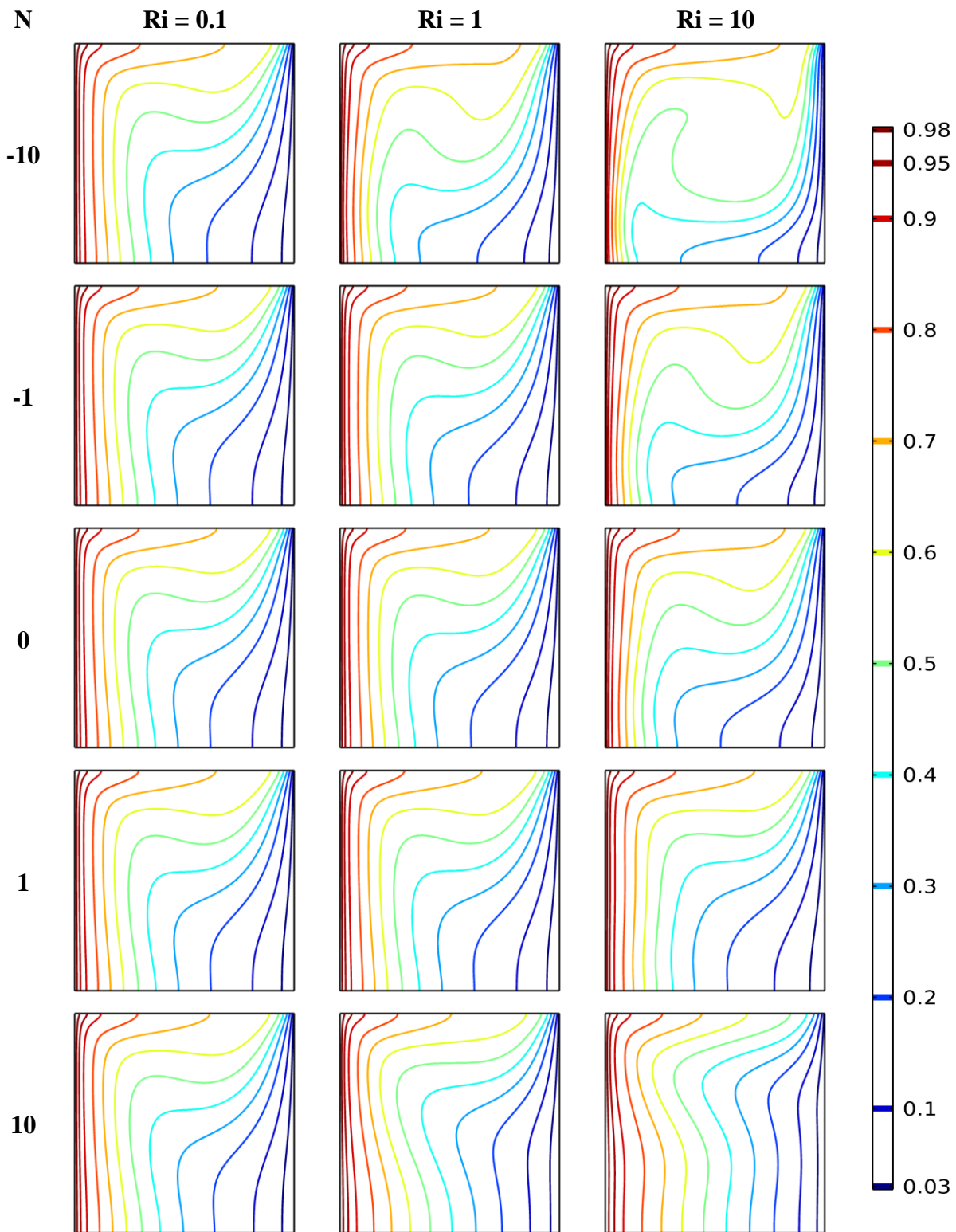


Fig. 3.10: Isotherm Plots for $Re = 10$, $Le = 1$ at $Ha = 0$.

Fig. 3.11 represents variation of the Iso-concentration contours for various values of Ri ($= 0.1, 1, 10$) and distinct magnitudes of N ($= -10$ to 10) at fixed values of $Re = 10$, $Le = 1$, and $Ha = 0$. Here, distribution of species transfer remains almost similar for all values of N together with different Ri values except for the cases of $N =$

-10, $Ri = 10$ and $N = 10$, $Ri = 10$. Since solute buoyancy force strongly resists the thermal one at $N = -10$, $Ri = 10$ leads to the enhancement in species transfer. On the other hand, the mass contours become almost flattered at the bottom and very middle of the cavity for $N = 10$, $Ri = 10$.

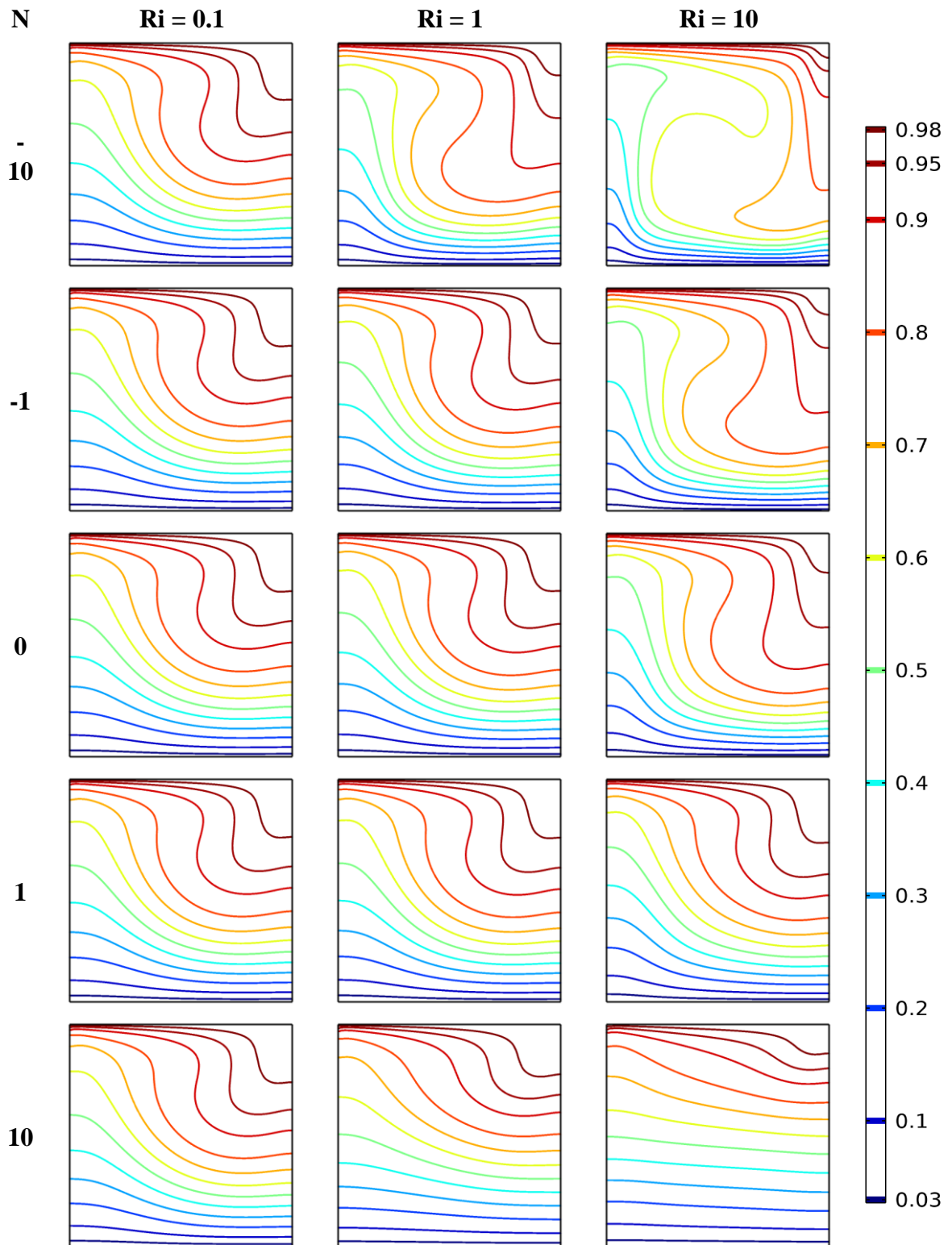


Fig. 3.11: Concentration Curves for $Re = 10$, $Le = 1$ at $Ha = 0$.

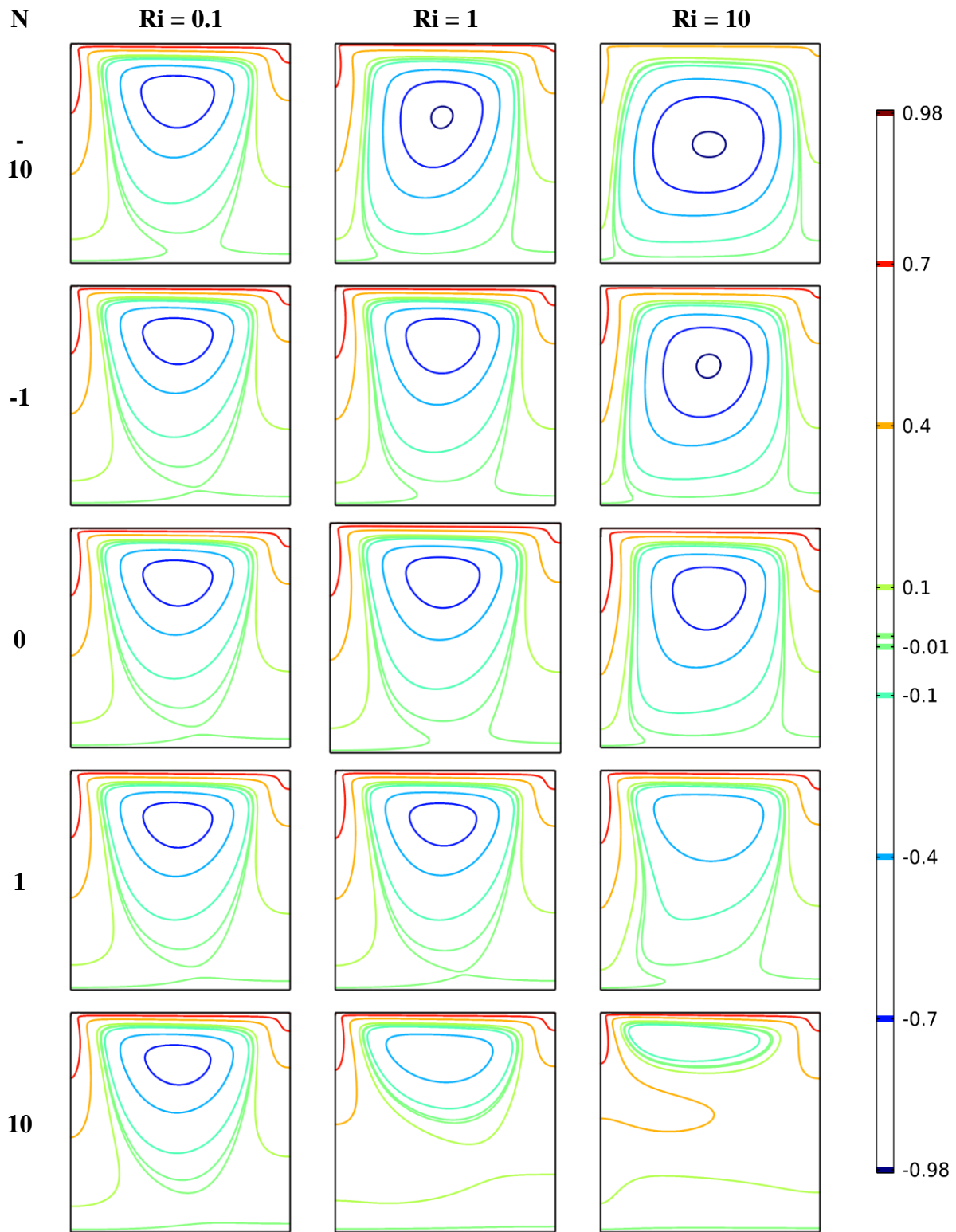


Fig. 3.12: Heat lines for $Re = 10$, $Le = 1$ at $Ha = 0$.

The distribution of heat lines for distinct values of Ri ($= 0.1, 1, 10$) and various magnitudes of N ($= -10$ to 10) at fixed values of $Re = 10$, $Le = 1$, and $Ha = 0$

is shown by Fig. 3.12. Clearly, the thermal energy transport pattern varies significantly for different values of Ri at a particular value of N . In such a context, it is important to note that solute buoyancy force counteracts thermal buoyancy force at a negative value of N . At $N=0$, only thermal buoyancy force exists. However, they become equal at $N=1$. Also, for the positive high value of N solute buoyancy forces dominate over the thermal one. Again, when Ri is increased from 0.1 to 10 then the flow of heat energy is reported through the free convective heat transport mechanism.

3.4 Effect of Variation of Ri and Ha

Fig. 3.13 depicts the variation of the streamlines for various values of Ri (= 0.1, 1, 10) together with distinct Ha figures (= 20, 40, 80) at constant values of $Re = 100$, $Le = 1$, and $N = 1$. It is noted that clockwise circulation is established within the cavity throughout the study range. With the increase of Ri at a particular value of Ha , major changes happen in the flow structure. At a low value of $Ha = 20$, the magnitude of Lorentz force is low and in such a situation buoyancy force dominates over the earlier. However, when the value of Ha is raised up to 40 and 80 then enhanced Lorentz force resists the fluid flow, leading to a decrement in the circulation strength.

The isotherm contours for various values of Ri (= 0.1, 1, 10) together with (= 20, 40, 80) at constant values of $Re = 100$, $Le = 1$, and $N = 1$ are presented by the Fig. 3.14. It is observed that temperature distribution within the cavity changes in a notable manner for different Ri values together with a particular value of Ha . At a low magnitude of $Ha = 20$ together with a higher value of $Ri = 10$, the natural convective heat transfer rules over the conduction mechanism. However, the reverse mechanism is noticed for a higher value of $Ha = 80$ at $Ri = 10$. This is due to the resistance imposed by the Lorentz force; generated by the external magnetic field against the buoyant forces.

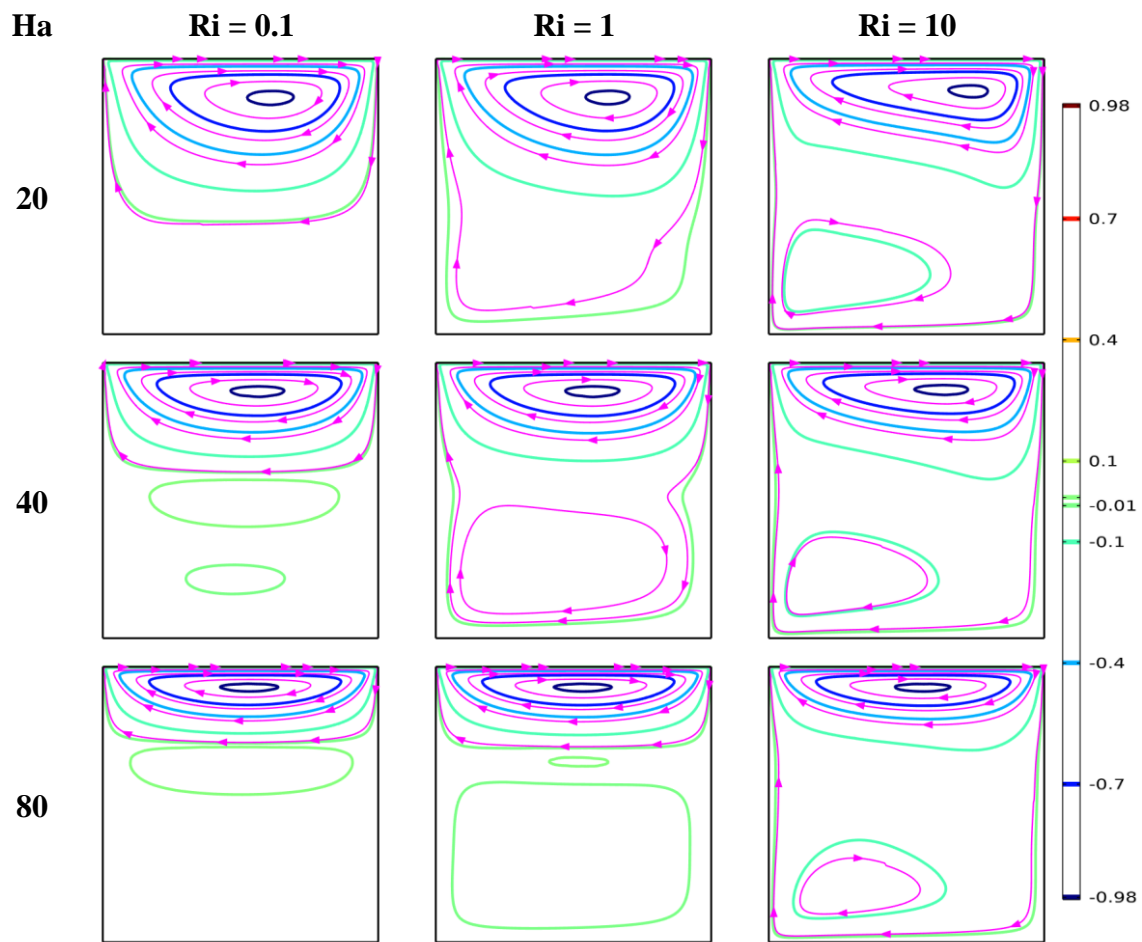


Fig. 3.13: Streamline Contours for $Re = 100$, $Le = 1$, and $N = 1$.

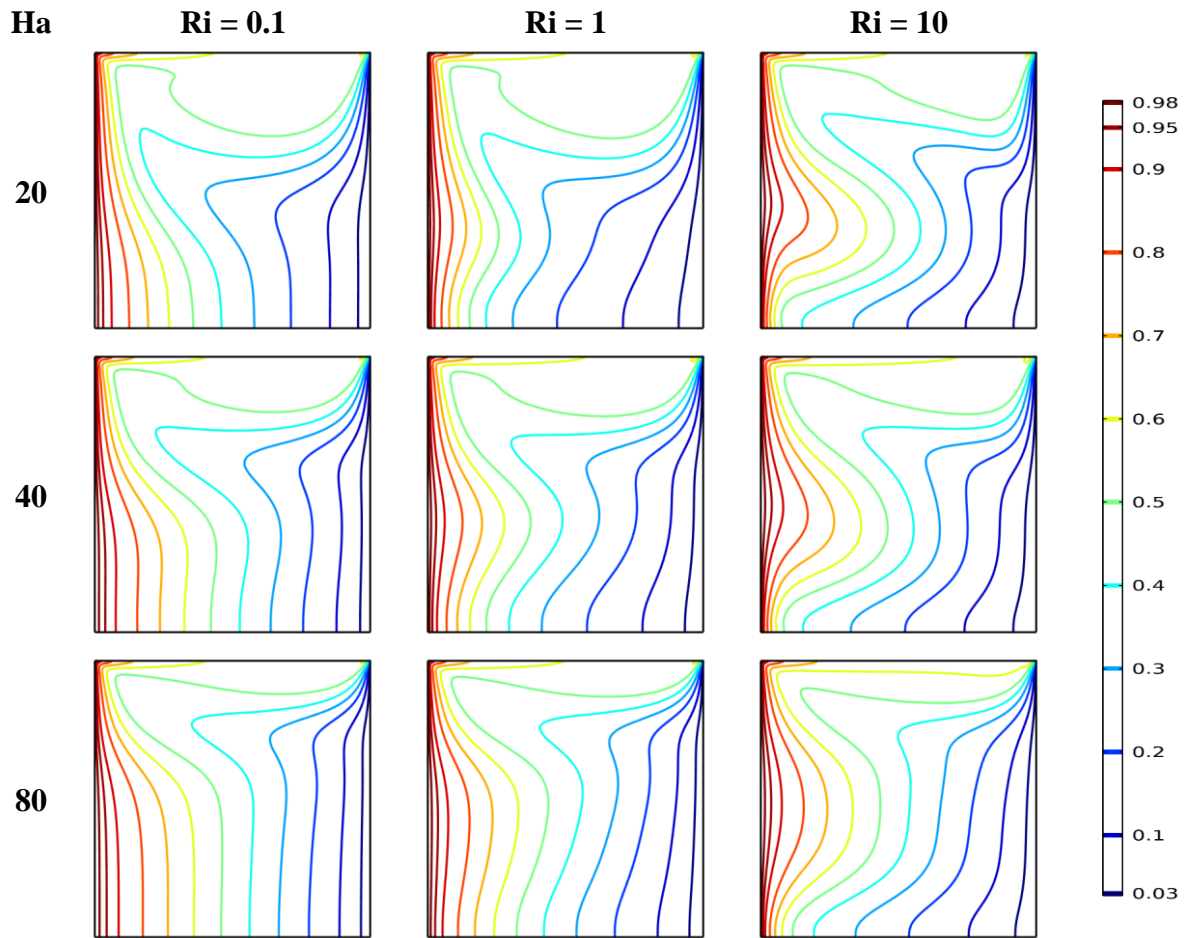


Fig. 3.14: Isotherm Plots for $Re = 100$, $Le = 1$, and $N = 1$.

Fig. 3.15 illustrates the variation of the iso-concentration contours for various values of Ri ($= 0.1, 1, 10$) together with distinct Ha figures ($= 20, 40, 80$) at constant values of $Re = 100$, $Le = 1$, and $N = 1$. It is observed that for the distinct values of Ha at $Ri = 0.1$, the concentration curves are flatter at the bottom and at the very middle of the cavity. However, they appear with non-linear behavior at both $Ri = 1$ and $Ri = 10$ for the different Ha values. It is important to mention here that at the high magnitude of Ha fluid flow is arrested, leading to the decrement in the mass transfer phenomena.

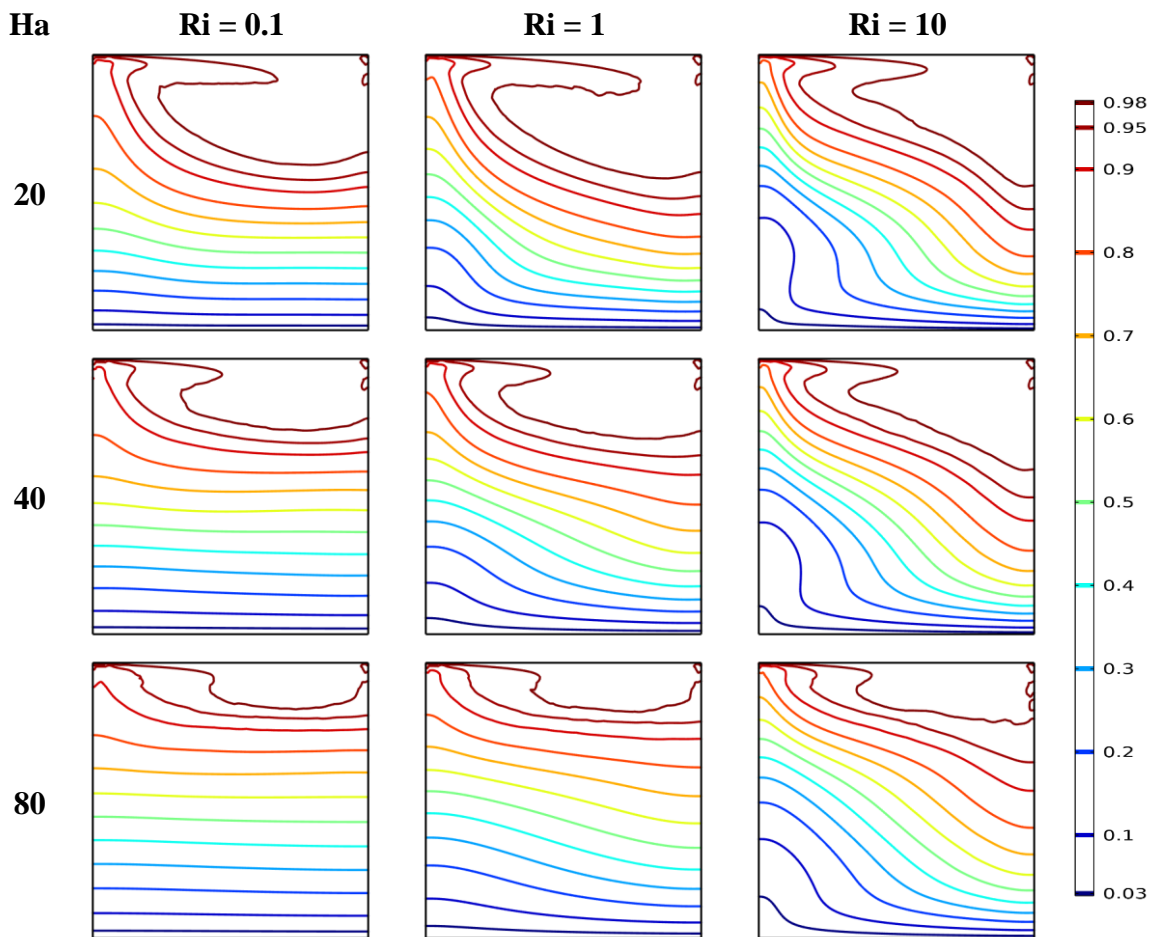


Fig. 3.15: Concentration Curves for $Re = 100$, $Le = 1$, and $N = 1$.

The heat lines for various values of Ri ($= 0.1, 1, 10$) together with ($= 20, 40, 80$) at constant values of $Re = 100$, $Le = 1$, and $N = 1$ are highlighted through the Fig. 3.16. It is noted that thermal energy distribution varies in a drastic way with different Ri values at a particular value of Ha . Further to the dampening effect is less at a low value of $Ha = 20$ but when Ha is raised to the high value say 80 then sufficient dampings is imposed to the heat energy density.

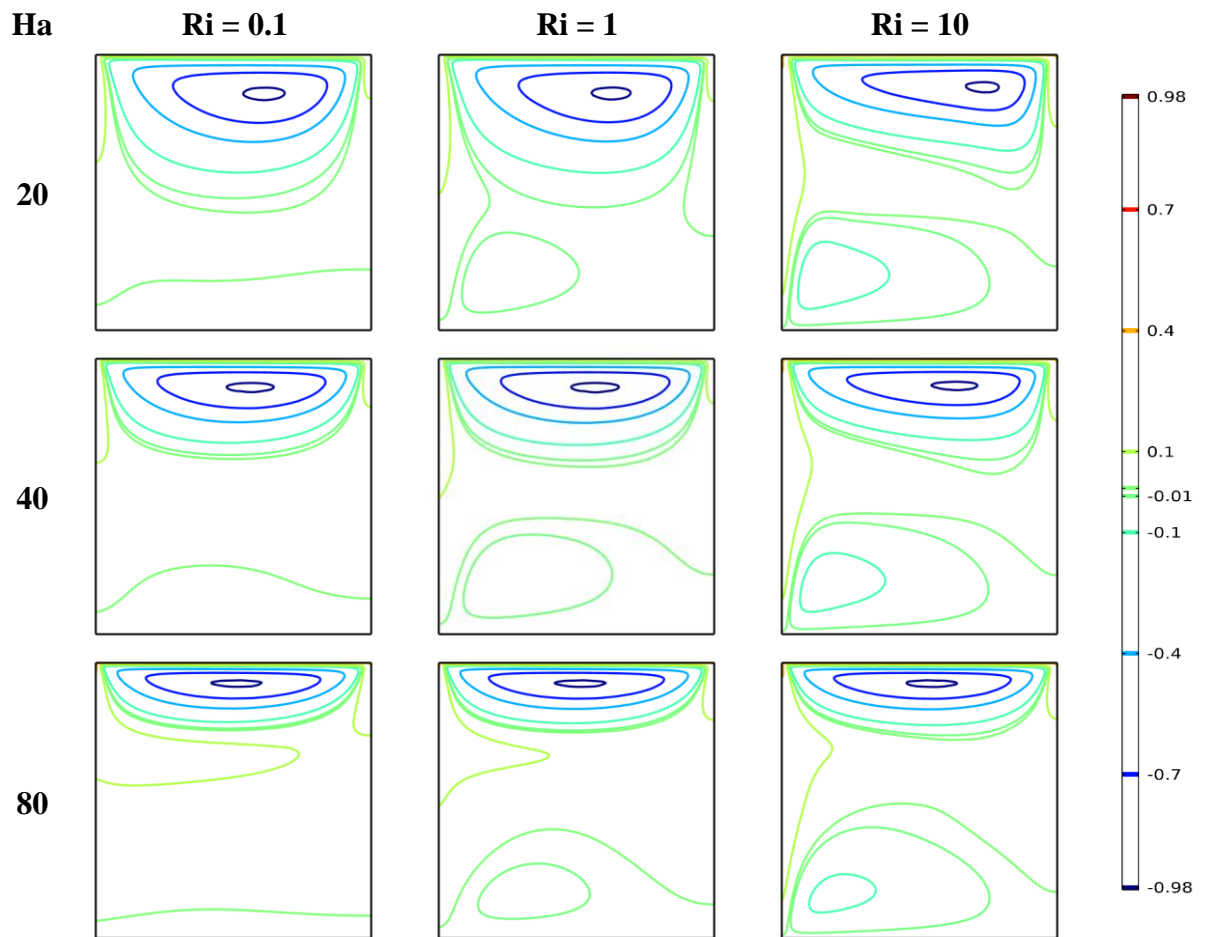


Fig. 3.16: Heat lines for $Re = 100$, $Le = 1$, and $N = 1$.

3.5 Heat and Mass Transfer Characteristics

The global parameters such as Average Nu and Average Sh represent heat and mass transfer features respectively and they are studied for a wide range of distinct study parameters Ri, Re, Le, N, and Ha. The relevant discussion is as given below:

Fig. 3.17 shows the variation of average Nu with various values of Re and Ri by keeping other parameters to be fixed. It is quite evident that Nu_{avg} increases with the increase of Re for various values of Ri taken. Further to this maximum average Nu = 5.5381 is noted for high value of Re = 100 at low value of Ri = 0.1. This is because at a high Re value, fluid velocity would be more and subsequently, heat transfer would be augmented as forced convection effects would be dominating over the free convection.

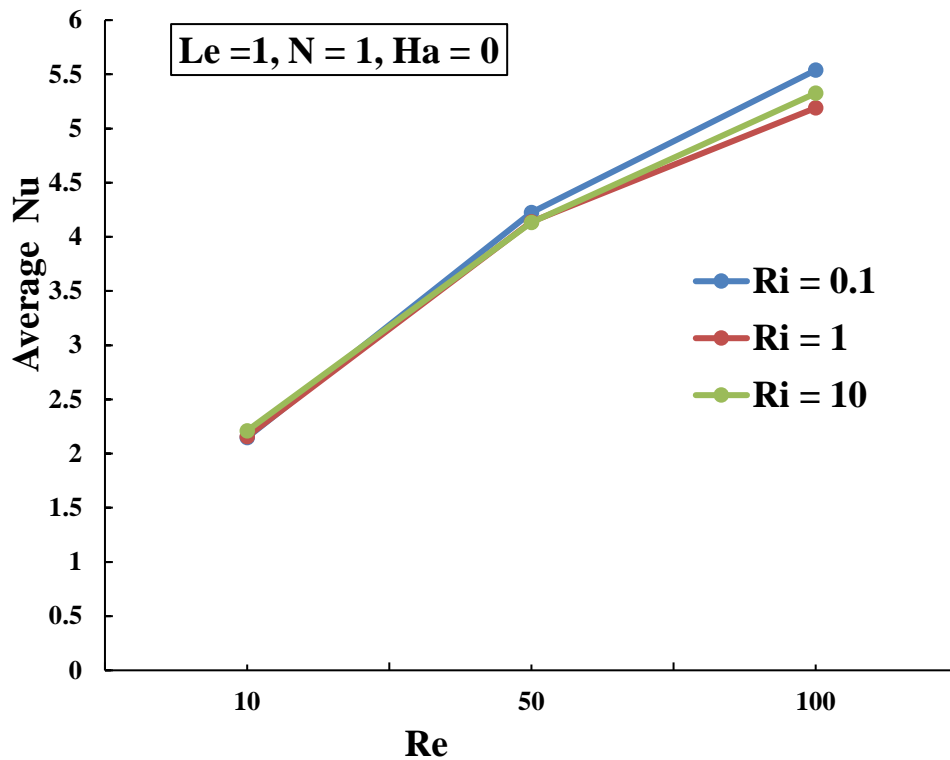


Fig. 3.17: Variation of Average Nu with Re and Ri for $Le = 1, N = 1, Ha = 0$.

Fig. 3.18 shows the variation of average Sh with various values of Re and Ri by keeping other parameters to be fixed. It is quite evident that Sh_{avg} increases with the increase of Re for various values of Ri taken. Further to this maximum average $Sh = 4.0278$ is noted for high value of $Re = 100$ at low value of $Ri = 0.1$. This is because at a high Re value, fluid velocity would be more and subsequently, species transfer would be enhanced.

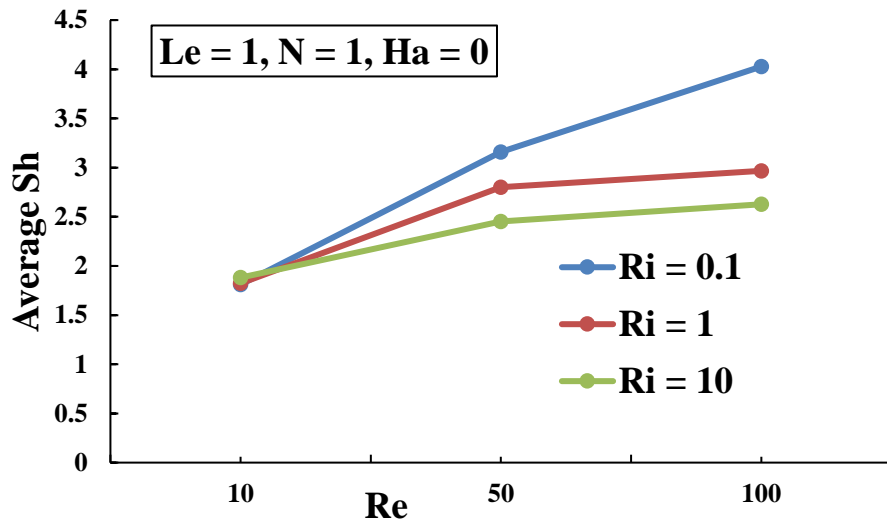


Fig. 3.18: Variation of Average Sh with Re and Ri for $Le = 1, N = 1, Ha = 0$.

Fig. 3.19 shows the variation of average Nu with various values of Le and Ri by keeping other parameters to be fixed. It is quite evident that Nu_{avg} increases with the increase of Le for various values of Ri taken. Further to the maximum average $Nu = 4.5064$ is observed for the high value of $Le = 5$ at a high value of $Ri = 10$. This is because at a high Le value, thermal diffusivity would be more and subsequently, heat transfer would be increased. However, it is noted that the free convection mode of heat transfer would be dominating over the forced one at a high Ri value.

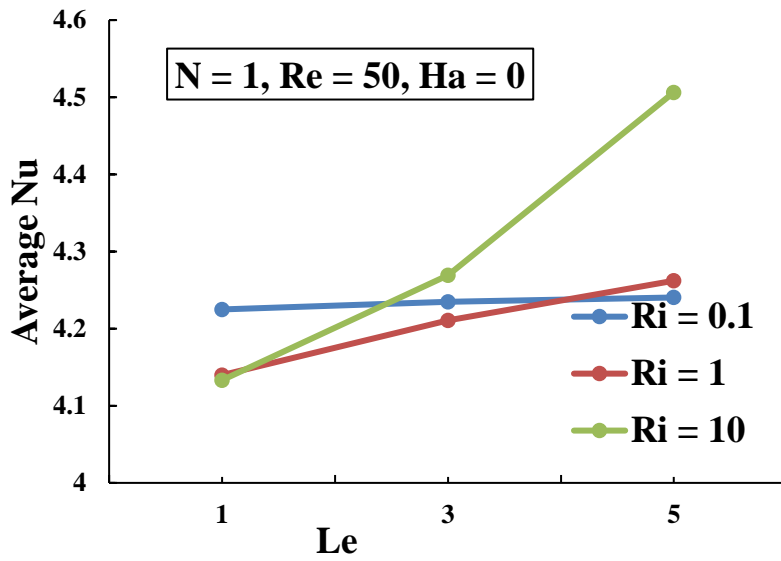


Fig. 3.19: Variation of Average Nu with Le and Ri for $N = 1$, $Re = 50$, $Ha = 0$.

Fig. 3.20 shows the variation of average Sh with various values of Le and Ri by keeping other parameters to be fixed. Clearly, Sh_{avg} rises with the rise of Le. However, Sh_{avg} decreases with the increase of Ri. Further to this maximum average, $Sh = 5.4501$ is observed for a high magnitude of $Le = 5$ at a low figure of $Ri = 0.1$. This is because, at a low Ri value, fluid velocity would be more, and subsequently, the associated mass transfer would be increased.

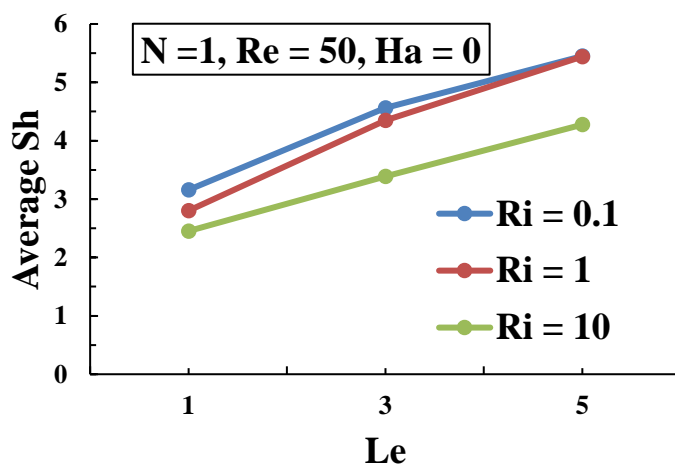


Fig. 3.20: Variation of Average Sh with Le and Ri for $N = 1$, $Re = 50$, $Ha = 0$.

Fig. 3.21 shows the variation of average Nu with different values of N and Ri by keeping other parameters to be fixed. It is obvious that Nu_{avg} decreases with the increase of N for various values of Ri taken. Further to the maximum average $Nu = 4.4102$ is noted for a negative value of $N = -10$ at high magnitude of $Ri = 10$. Since at a high N value, solute buoyancy force dominates over thermal buoyancy force and a negative value of N the previous one counteracts the last one. Also, at a high value of Ri free convection is the governing mode of heat transfer.

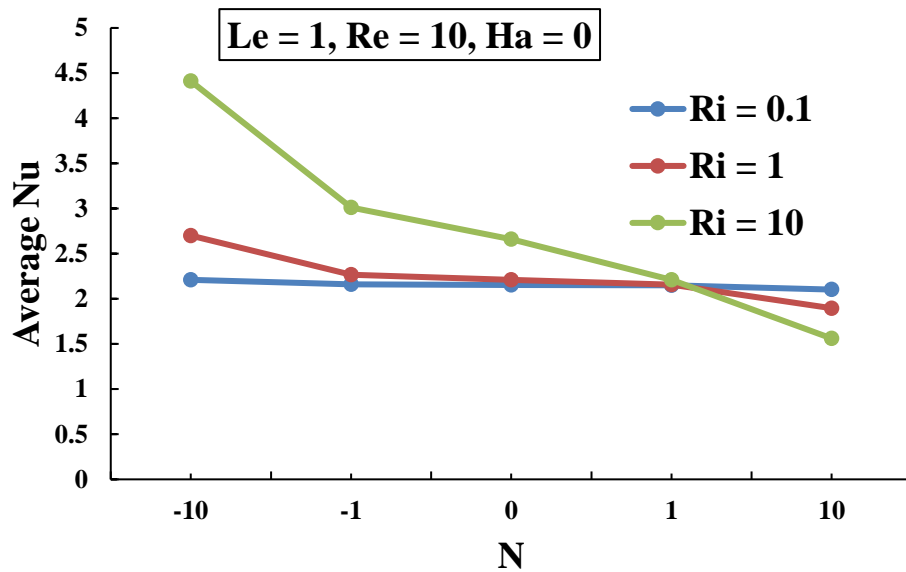


Fig. 3.21: Variation of Average Nu with N and Ri for $Le = 1$, $Re = 10$, $Ha = 0$.

Fig. 3.22 shows the variation of average Sh with various values of N and Ri by keeping other parameters to be fixed. It is quite evident that Sh_{avg} decreases with the increase of N for various values of Ri taken. Further to this maximum average $Sh = 4.3188$ is attained the negative value of $N = -10$ at the high magnitude of $Ri = 10$. Since at a high N value, solute buoyancy force dominates over thermal buoyancy force and at a negative value of N, the previous one counteracts the last one.

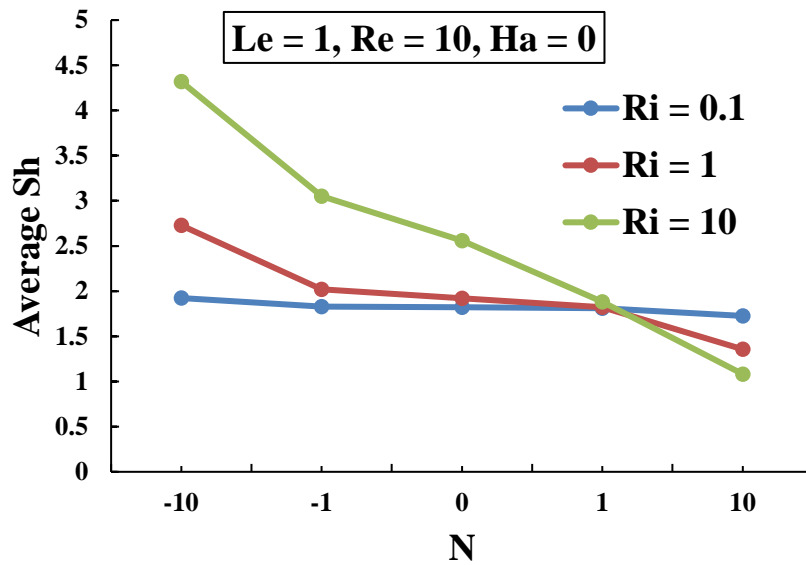


Fig. 3.22: Variation of Average Sh with N and Ri for $Le = 1$, $Re = 10$, $Ha = 0$.

Fig. 3.23 shows the variation of average Nu with various values of Ha and Ri by keeping other parameters to be fixed. Evidently, Nu_{avg} decreases with the increase of Ha for various values of Ri taken. As with the increase of Ha, Lorentz force enhance which counteracts associated buoyant forces. In view of the same, the maximum average $Nu = 5.5381$ is obtained in the absence of a magnetic field ($Ha = 0$) at a low value of $Ri = 0.1$. Also, at a low Ri value, fluid velocity would be more, and subsequently, heat transfer would be enhanced as forced convection effects would be dominating over the free convection.

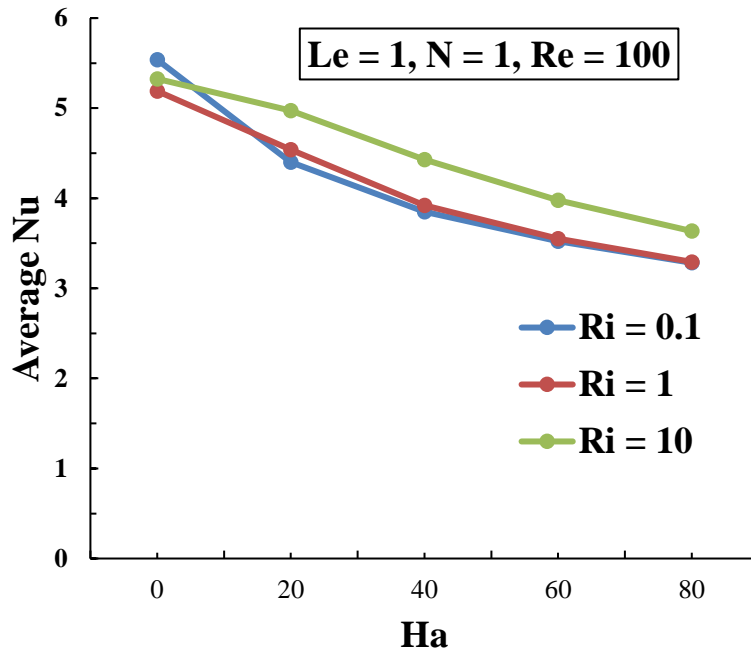


Fig. 3.23: Variation of Average Nu with Ha and Ri for Le = 1, N = 1, Re = 100.

Fig. 3.24 shows the variation of average Sh with various values of Ha and Ri by keeping other parameters to be fixed. Evidently, Sh_{avg} decreases with the increase of Ha for various values of Ri taken. As with the increase of Ha, Lorentz force enhance which counteracts associated buoyant forces. In view of the same, maximum average Sh = 4.0278 is obtained in the absence of a magnetic field (Ha = 0) at a low value of Ri = 0.1

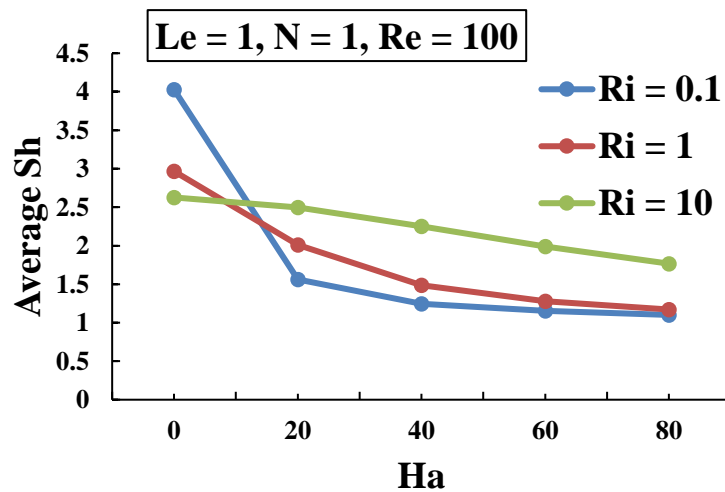


Fig. 3.24: Variation of Average Sh with Ha and Ri for Le = 1, N = 1, Re = 100.

3.6 Conclusions

The current numerical work is established by considering the Galerkin's finite element iterative method for the solution of steady thermo-solute gravity-induced laminar and mixed convective flow regime of H₂O within a square enclosure subjected to differential heating and concentration under magnetic and non-magnetic effects. Here, the phenomena of fluid flow, heat flow, and mass flow within the cavity is demonstrated by utilizing the effect of relevant study parameters such as Re, Ri, Le, N, and Ha with their wide range of variations on streamline contours, isotherm curves, iso-concentration plots, and Heat line contours as well. Also, the study reveals for the parametric figures at which the optimum heat and mass transfer within the computing geometry would be attained as indicated by the maximum value of Nu_{avg} and Sh_{avg} successively. The major outcomes of the present research work are summarised as shown below:

- a) It is observed that Nu_{avg} increases with the increase of Re for various values of Ri at $Le = 1$, $N = 1$, $Ha = 0$. Also, maximum value of $Nu_{avg} = 5.5381$ is noticed at $Re = 100$, $Ri = 0.1$. Here, forced convection is the governing mode of thermo-solutal transport.
- b) Sh_{avg} enhances with the rise of Re for various values of Ri at $Le = 1$, $N = 1$, $Ha = 0$. Consequently, maximum average $Sh = 4.0278$ is obtained at $Re = 100$, $Ri = 0.1$.
- c) It is concluded that average Nu increases with the increase of Le for various values of Ri at $N = 1$, $Re = 50$, $Ha = 0$. Here, the maximum average $Nu = 4.5064$ is reported $Le = 5$ at $Ri = 10$ and the natural convection mode of heat transfer would be dominating over the forced convection effects.
- d) It is observed that average Sh rises with the rise of Le and decreases with the increase of Ri at $N = 1$, $Re = 50$, $Ha = 0$. Thus, average $Sh = 5.4501$ is attained for $Le = 5$ at $Ri = 0.1$.
- e) Nu_{avg} decreases with the increase of N for various values of Ri at $Le = 1$, $Re = 10$, $Ha = 0$. Again, average $Nu = 4.4102$ is noted for $N = -10$ at $Ri = 10$.
- f) Average Sh decreases with the increase of N for various values of Ri Further to this maximum average $Sh = 4.3188$ is attained negative value of $N = -10$ at high magnitude of $Ri = 10$ at $Le = 1$, $Re = 10$, $Ha = 0$.

- g) It is found that Nu_{avg} decreases with the increase of Ha for various values of Ri at $N = 1$, $Le = 1$, $Re = 100$. Ultimately, maximum average $Nu = 5.5381$ is obtained for $Ha = 0$ at $Ri = 0.1$. As with the rise of Ha , the increased Lorentz force opposes the buoyant forces.
- h) Sh_{avg} reduces with the rise of Ha for various values of Ri at $N = 1$, $Le = 1$, $Re = 100$ and maximum average $Sh = 4.0278$ is achieved for $Ha = 0$ at $Ri = 0.1$.

From the above outcomes, finally it can be concluded that optimum thermal transport phenomena within the geometry is noticed under the parametric conditions of $Re = 100$, $Ri = 0.1$, $Le = 1$, $N = 1$, and $Ha = 0$ at which $Nu_{avg} = 5.5381$. Further to that, optimum species transfer within the cavity is established under the parametric conditions of $Re = 50$, $Ri = 0.1$, $Le = 5$, $N = 1$, and $Ha = 0$ at which $Sh_{avg} = 5.4501$. The findings of this study will enrich the knowledge on the thermo-solutal transport process.

CHAPTER – 4

Scope of Future Work

As dual diffusion hybrid convection mechanism is frequently observed in the nature, various domains of science and engineering, and a lot of industries. Although, it is an extremely complicated thermo-solute transport phenomenon. In the past, several studies were conducted on it numerically as well as experimentally. Also, plenty of the research work is going on the subject topic of interest by multiple investigators nowadays.

In the current study, we have limited our attention on the 2-D, steady, laminar combined heat and mass transfer convective flow problem involving differentially heated-concentrated classical lid-driven square cavity comprising of H₂O as the working media imposed to both magnetic and non-magnetic effects by performing numerical verification.

In view of the above, this steady mode of study can be further extended in the upcoming future works by implementing the distinct conceptions such as 3D, unsteady, and turbulent flow regime, several working substances (air, nano-liquids, porous media, non-Newtonian fluids), complicated geometries, non-uniform boundary conditions of heating and concentration, mass line analysis and entropy evolution phenomena within the computational domain of interest.

Furthermore, the investigation could be extended by designing a suitable experimental setup involving various multiphysical scenarios. In fact, the mixed convective double-diffusive transport process could be explored by adopting free aspiration of the surrounding fluids, which will provide more insights into the practical application process.

References

- [1] Al-Amiri, Abdalla M., Khalil Khanafer and Ioan Pop. "Numerical simulation of combined thermal and mass transport in a square lid-driven cavity." *International Journal of Thermal Sciences* 46 (2007): 662-671.
- [2] Teamah, Mohamed A. and Wael M. El-Maghlany. "Numerical simulation of double-diffusive mixed convective flow in rectangular enclosure with insulated moving lid." *International Journal of Thermal Sciences* 49 (2010): 1625-1638.
- [3] Teamah, Mohamed A., Medhat M. Sorour, Wael M. El-Maghlany and Amr N. Afifi. "Numerical simulation of double diffusive laminar mixed convection in shallow inclined cavities with moving lid." *Alexandria Engineering Journal* 52 (2013): 227-239.
- [4] Qin, Qiao, Zhongjia Xia and Zhen F. Tian. "High accuracy numerical investigation of double-diffusive convection in a rectangular enclosure with horizontal temperature and concentration gradients." *International Journal of Heat and Mass Transfer* 71 (2014): 405-423.
- [5] Chen, Sheng, Hao Liu and Chuguang Zheng. "Numerical study of turbulent double-diffusive natural convection in a square cavity by LES-based lattice Boltzmann model." *International Journal of Heat and Mass Transfer* 55 (2012): 4862-4870.
- [6] Rahman, Mustafizur, Hakan F. Oztop, Amimul Ahsan, Md. Abul Kalam and Yasin Varol. "Double-diffusive natural convection in a triangular solar collector." *International Communications in Heat and Mass Transfer* 39 (2012): 264-269.
- [7] Corcione, Massimo, Stefano Grignaffini and Alessandro Quintino. "Correlations for the double-diffusive natural convection in square enclosures induced by opposite temperature and concentration gradients." *International Journal of Heat and Mass Transfer* 81 (2015): 811-819.
- [8] Nazari, Mohsen, Ladan Louhghalam and M. H. Kayhani. "Lattice Boltzmann simulation of double diffusive natural convection in a square cavity with a hot square obstacle." *Chinese Journal of Chemical Engineering* 23 (2015): 22-30.
- [9] Koufi, Lounes, Yassine Cherif, Zohir Younsi and Hassane Naji. "Double-Diffusive Natural Convection in a Mixture-Filled Cavity with Walls' Opposite

- Temperatures and Concentrations.” *Heat Transfer Engineering* 40 (2019): 1268 - 1285.
- [10] Arun, S., A. Satheesh and Ali J. Chamkha. “Numerical Analysis of Double-Diffusive Natural Convection in Shallow and Deep Open-Ended Cavities Using Lattice Boltzmann Method.” *Arabian Journal for Science and Engineering* 45 (2019): 861-876.
- [11] Said, K. Ait, Ahmed Ouadha and Amina Sabeur. “CFD-based analysis of entropy generation in turbulent double diffusive natural convection flow in square cavity.” *MATEC Web of Conferences* (2020).
- [12] Ghernoug, Chahinez, Mahfoud Djeddar, Hassane Naji and Abdelkarim Bouras. “Towards numerical computation of double-diffusive natural convection within an eccentric horizontal cylindrical annulus.” *International Journal of Numerical Methods for Heat and Fluid Flow* 26 (2016): 1346-1364.
- [13] Taloub, Djedid, Abdelkarim Bouras, Mahfoud Djeddar and Zied Driss. “Numerical research of double-diffusive natural convection in elliptical cylinders: Effect of thermal Rayleigh number.” *Heat Transfer* 49 (2020): 2194 - 2205.
- [14] Al-Farhany, K., Mohammed Azeez Alomari, Khalid B. Saleem, Wael G Al-Kouz and Nirmalendu Biswas. “Numerical investigation of double-diffusive natural convection in a staggered cavity with two triangular obstacles.” *The European Physical Journal Plus* (2021).
- [15] Eshaghi, Soroush, Farhad Izadpanah, A. Sattar Dogonchi, Ali J. Chamkha, Mohamed Bechir Ben Hamida and Hesham Alhumade. “The optimum double diffusive natural convection heat transfer in H-Shaped cavity with a baffle inside and a corrugated wall.” *Case Studies in Thermal Engineering* (2021).
- [16] Moolya, Shivananda and A. Satheesh. “Role of magnetic field and cavity inclination on double diffusive mixed convection in rectangular enclosed domain.” *International Communications in Heat and Mass Transfer* 118 (2020): 104814.
- [17] Moolya, Shivananda and Satheesh Anbalgan. “Optimization of the effect of Prandtl number, inclination angle, magnetic field, and Richardson number on double-diffusive mixed convection flow in a rectangular domain.” *International Communications in Heat and Mass Transfer* (2021).

- [18] Teamah, Mohamed A. and Ali I. Shehata. "Magnetohydrodynamic double diffusive natural convection in trapezoidal cavities." *alexandria engineering journal* 55 (2016): 1037-1046.
- [19] Maatki, Chemseddine, Kaouther Ghachem, Lioua Kolsi, Ahmed Kadhim Hussein, Mohamed Naceur Borjini and Habib Ben Aissia. "Inclination effects of magnetic field direction in 3D double-diffusive natural convection." *Appl. Math. Comput.* 273 (2016): 178-189.
- [20] Maatki, Chemseddine, Walid Hassen, Lioua Kolsi, Naif G. M. Alshammari, Mohamed Naceur Borjini and Habib Ben Aissia. "3-D Numerical Study of Hydromagnetic Double Diffusive Natural Convection and Entropy Generation in Cubic Cavity." *Journal of Applied Fluid Mechanics* 9 (2016): 1915-1925.
- [21] Mondal, Sabyasachi and Precious Sibanda. "An Unsteady Double-Diffusive Natural Convection in an Inclined Rectangular Enclosure with Different Angles of Magnetic Field." *International Journal of Computational Methods* 13 (2015): 1641015.
- [22] Reddy, Nithish and K. Murugesan. "Magnetic field influence on double-diffusive natural convection in a square cavity – A numerical study." *Numerical Heat Transfer, Part A: Applications* 71 (2017): 448 - 475.
- [23] Venkatadria, K., S. Gouse Mohiddina and M. Suryanarayana Reddyb. "mathematical modelling of unsteady mhd double- diffusive natural convection flow in a square cavity." (2017).
- [24] Sathiyamoorthi, Arun and Satheesh Anbalagan. "Mesoscopic analysis of heatline and massline during double-diffusive MHD natural convection in an inclined cavity." *Chinese Journal of Physics* (2018).
- [25] Mahapatra, T. Ray and Priyajit Mondal. "Heatline and Massline Analysis Due to Magnetohydrodynamic Double Diffusive Natural Convection in a Trapezoidal Enclosure with Various Aspect Ratios." *International Journal of Applied and Computational Mathematics* 5 (2019): 1-26.
- [26] Mojumder, Satyajit, Sourav Saha, Sumon Saha, Rezwana Rahman and Suvash Chandra Saha. "Effect of Magnetic Field on Double Diffusive Natural Convection Inside a Square Cavity with Isothermal Hollow Insert." *IOP Conference Series: Materials Science and Engineering* (2020).

- [27] Mondal, Priyajit and T. Ray Mahapatra. "MHD double-diffusive mixed convection and entropy generation of nanofluid in a trapezoidal cavity." *International Journal of Mechanical Sciences* 208 (2021): 106665.
- [28] Shah, Syed Saqib, Rizwan Ul Haq and Wael G Al-Kouz. "Mixed convection analysis in a split lid-driven trapezoidal cavity having elliptic shaped obstacle." *International Communications in Heat and Mass Transfer* (2021).
- [29] Esfahani, Javad Abolfazli and Vahid Bordbar. "Double Diffusive Natural Convection Heat Transfer Enhancement in a Square Enclosure Using Nanofluids." *Journal of Nanotechnology in Engineering and Medicine* 2 (2011): 021002.
- [30] Sheikhzadeh, Ghanbar Ali, Majid Dastmalchi and H. Khorasanizadeh. "Effects of walls temperature variation on double diffusive natural convection of Al₂O₃-water nanofluid in an enclosure." *Heat and Mass Transfer* 49 (2013): 1689-1700.
- [31] Chen, Sheng, Bo Yang, Xiao Xiao and Chuguang Zheng. "Analysis of entropy generation in double-diffusive natural convection of nanofluid." *International Journal of Heat and Mass Transfer* 87 (2015): 447-463.
- [32] Chowdhury, Raju, Salma Parvin and Md. Abdul H. Khan. "Numerical Study of Double-diffusive Natural Convection in a Window Shaped Cavity Containing Multiple Obstacles Filled with Nanofluid." *Procedia Engineering* 194 (2017): 471-478.
- [33] Abidi, Awatef, Zehba A. S. Raizah and Jamel Madiouli. "Magnetic Field Effect on the Double Diffusive Natural Convection in Three-Dimensional Cavity Filled with Micropolar Nanofluid." *Applied Sciences* (2018).
- [34] Ali, Mohammad Mokaddes, M. A. Alim and Rehena Nasrin. "Effect of magnetic field on double diffusive natural convection flow in a closed chamber using nanofluid." (2018).
- [35] Mahapatra, T. Ray, Bikash Chandra Saha and Dulal Pal. "Magnetohydrodynamic double-diffusive natural convection for nanofluid within a trapezoidal enclosure." *Computational and Applied Mathematics* 37 (2018): 6132-6151.
- [36] Saha, Bikash Chandra, T. Ray Mahapatra and Dulal Pal. "Analysis of Heatline and Massline in Magnetohydrodynamic Double Diffusive Natural Convection of Nanofluid Within a Trapezoidal Enclosure." *Journal of Nanofluids* (2018).

- [37] Saritha, Natesan and A. Senthil Kumar. “Double diffusive natural convection in a square enclosure filled with copper-water nanofluid induced by opposite temperature and concentration gradients.” *Computational Thermal Sciences: An International Journal* 10 (2018): 307-320.
- [38] Manaa, Nessrin, Awatef Abidi, Ahamed Saleel C., Salha Mohammed Al Makwash and Mohammed Naceur Borjini. “On Simulation of Double-Diffusive Natural Convection in a Micropolar Nanofluid Filled Cubic Cavity.” *Heat Transfer Engineering* 42 (2020): 947 - 965.
- [39] Al-Balushi, Latifa M., Md. J. Uddin, Mohammad M. Rahman, Hakan F. Oztop and Ioan Pop. “Three-dimensional tilted hydromagnetic natural double-diffusive convection in a rectangular cuboid filled with nanofluids based on magnetic nanoparticles.” *Heat Transfer* 51 (2021): 1275 - 1305.
- [40] Umavathi, Jawali C., Bernardo Buonomo, Oronzio Manca and Mikhail A. Sheremet. “Double diffusion in a rectangular duct using metals or oxides suspended in a viscous fluid.” *Thermal science and engineering* 21 (2021): 100793.
- [41] Uddin, M. Borhan, M. M. Rahman, Mahram Khan, Rahman Saidur and Talaat A. Ibrahim. “Hydromagnetic double-diffusive mixed convection in trapezoidal enclosure due to uniform and nonuniform heating at the bottom side: Effect of Lewis number.” *alexandria engineering journal* 55 (2016): 1165-1176.
- [42] Nath, Ratnadeep and K. Murugesan. “Double diffusive mixed convection in a Cu-Al₂O₃/water nanofluid filled backward facing step channel with inclined magnetic field and part heating load conditions.” *Journal of Energy Storage* (2021).
- [43] Gholizadeh, Mohammad, Rasoul Nikbakhti, Javad Khodakhah and Amirmahdi Ghasemi. “Numerical study of double diffusive buoyancy forces induced natural convection in a trapezoidal enclosure partially heated from the right sidewall.” *alexandria engineering journal* 55 (2016): 779-795.
- [44] Parvin, Salma, Rehena Nasrin, M. A. Alim and Nazmul Hossain. “Double-diffusive natural convection in a partially heated enclosure using a nanofluid.” *Heat Transfer Research* 41 (2012): 484-497.
- [45] Nikbakhti, Rasoul and Asgar Bradaran Rahimi. “Double-Diffusive Natural Convection In A Rectangular Cavity With Partially Thermally Active Side

- Walls.” *Journal of The Taiwan Institute of Chemical Engineers* 43 (2012): 535-541.
- [46] Mahapatra, T. Ray, Dulal Pal and Sabyasachi Mondal. “Effects of buoyancy ratio on double-diffusive natural convection in a lid-driven cavity.” *International Journal of Heat and Mass Transfer* 57 (2013): 771-785.
- [47] Arani, Ali Akbar Abbasian, E. Kakoli and Najmeh Hajjaligol. “Double-diffusive natural convection of Al₂O₃-water nanofluid in an enclosure with partially active side walls using variable properties.” *Journal of Mechanical Science and Technology* 28 (2014): 4681-4691.
- [48] Ghaffarpasand, Omid. “Massline Visualization of Double-Diffusive Natural Convection inside a Cavity Filled with Nanofluid Subjected to Heat Flux and Transverse Magnetic Field.” *Journal of Applied Fluid Mechanics* 10 (2017): 1427-1440.
- [49] He, Boyu, Shihua Lu, Dongyan Gao, Weiwei Chen and Xinjun Li. “Lattice Boltzmann simulation of double diffusive natural convection of nanofluids in an enclosure with heat conducting partitions and sinusoidal boundary conditions.” *International Journal of Mechanical Sciences* (2019).
- [50] Parveen, Rujda and T. Ray Mahapatra. “Numerical simulation of MHD double diffusive natural convection and entropy generation in a wavy enclosure filled with nanofluid with discrete heating.” *Heliyon* 5 (2019).
- [51] Afzalabadi, Abolfazl, Vahid Bordbar and Mohammad Ali Amooie. “Lattice Boltzmann simulation of magneto-hydrodynamic double-diffusive natural convection in an enclosure with internal heat and solute source using nanofluids.” *SN Applied Sciences* (2020).
- [52] Lu, Shihua, Boyu He, Dongyan Gao, Weiwei Chen and Xinjun Li. “Numerical simulation of double-diffusive natural convection in an enclosure in the presence of magnetic field with heat-conducting partition using lattice Boltzmann method.” *Journal of Thermal Analysis and Calorimetry* (2020): 1-18.
- [53] Parveen, Rujda, Priyajit Mondal and T. Ray Mahapatra. “Double Diffusive Magnetohydrodynamic (MHD) Natural Convection and Entropy Generation in a Discretely Heated Inclined Dome-Shaped Enclosure Filled with Cu-Water Nanofluid.” *Journal of Nanofluids* (2021).

- [54] Khan, Zafar Hayat, Waqar Ahmed Khan, Muhammad Qasim and Min Du. "Double-diffusive flow in a porous right-angle trapezoidal enclosure with constant heat flux." (2020).
- [55] Moukalled, F. and Marwan Darwish. "Double Diffusive Natural Convection in a Porous Rhombic Annulus." *Numerical Heat Transfer, Part A: Applications* 64 (2013): 378 - 399.
- [56] Mondal, Sabyasachi and Precious Sibanda. "Effects of buoyancy ratio on unsteady double-diffusive natural convection in a cavity filled with porous medium with non-uniform boundary conditions." *International Journal of Heat and Mass Transfer* 85 (2015): 401-413.
- [57] Chowdhury, Raju, Salma Parvin and Md. Abdul H. Khan. "Finite element analysis of double-diffusive natural convection in a porous triangular enclosure filled with Al₂O₃-water nanofluid in presence of heat generation." *Heliyon* 2 (2016).
- [58] Hadidi, Nasser and Rachid Bennacer. "Three-dimensional double diffusive natural convection across a cubical enclosure partially filled by vertical porous layer." *International Journal of Thermal Sciences* 101 (2016): 143-157.
- [59] Stajanko, Janja Kramer, Jure Ravnik and Renata Jecl. "Numerical simulation of three-dimensional double-diffusive natural convection in porous media by boundary element method." *Engineering Analysis With Boundary Elements* 76 (2017): 69-79.
- [60] Xu, Hongtao, T. T. Wang, Zhiguo Qu, Jiaying Chen and B. B. Li. "Lattice Boltzmann simulation of the double diffusive natural convection and oscillation characteristics in an enclosure filled with porous medium." *International Communications in Heat and Mass Transfer* 81 (2017): 104-115.
- [61] Li, Po-Wei, Wen Chen, Zhuojia Fu and C. M. Fan. "Generalized finite difference method for solving the double-diffusive natural convection in fluid-saturated porous media." *Engineering Analysis with Boundary Elements* (2018).
- [62] Al-Farhany, K. and Ali Turan. "Double-Diffusive of Natural Convection in an Inclined Porous Square Domain Generalized Model." *Al-Qadisiyah Journal for Engineering Sciences* (2019).

- [63] Saha, Bikash Chandra, T. Ray Mahapatra and Dulal Pal. "Simulation of Heatlines and Masslines Visualization of MHD Double-Diffusive Natural Convection in Al₂O₃-Nanofluid Saturated with Porous Medium." *Journal of Nanofluids* (2018).
- [64] Wang, Bo, Yi Liu and Ling Li. "Nanofluid double diffusive natural convection in a porous cavity under multiple force fields." *Numerical Heat Transfer, Part A: Applications* 77 (2019): 343 - 360.
- [65] Habibi, Mohammad Reza and Iman Zahmatkesh. "DOUBLE-DIFFUSIVE NATURAL AND MIXED CONVECTION OF BINARY NANOFLUIDS IN POROUS CAVITIES." *Journal of Porous Media* 23 (2020): 955-967.
- [66] He, Boyu, Shihua Lu, Dongyan Gao, Weiwei Chen and Fu-Min Lin. "Lattice Boltzmann simulation of double diffusive natural convection in heterogeneously porous media of a fluid with temperature-dependent viscosity." *Chinese Journal of Physics* 63 (2020): 186-200.
- [67] Marzougui, Souad, Ali Mchirgui and Mourad Magherbi. "DOUBLE DIFFUSIVE NATURAL CONVECTION AND ENTROPY GENERATION THROUGH A TRAPEZOIDAL POROUS CAVITY." *Special Topics and Reviews in Porous Media - An International Journal* 11 (2020): 189-202.
- [68] Reddy, E. S., Satyananda Panda, Manoj Kumar Nayak and O. Makinde. "Cross flow on transient double-diffusive natural convection in inclined porous trapezoidal enclosures." *Heat Transfer* 50 (2020): 849 - 875.
- [69] Vijaybabu, T. R.. "Influence of porous circular cylinder on MHD double-diffusive natural convection and entropy generation." *International Journal of Mechanical Sciences* 206 (2021): 106625.
- [70] Tizakast, Youssef, Mourad Kaddiri and Mohamed Lamsaadi. "Double-diffusive mixed convection in rectangular cavities filled with non-Newtonian fluids." *International Journal of Mechanical Sciences* 208 (2021): 106667.
- [71] Kefayati, Gh.R.. "Double-diffusive natural convection and entropy generation of Bingham fluid in an inclined cavity." *International Journal of Heat and Mass Transfer* 116 (2018): 762-812.
- [72] Kefayati, Gh.R.. "Lattice Boltzmann simulation of double-diffusive natural convection of viscoplastic fluids in a porous cavity." *Physics of Fluids* (2019).
- [73] Hussain, Shafqat, Shahin Shoeibi and Taher Armaghani. "Impact of magnetic field and entropy generation of Casson fluid on double diffusive natural

- convection in staggered cavity.” *International Communications in Heat and Mass Transfer* 127 (2021): 105520.
- [74] Makayssi, T., Mohamed Lamsaadi and Mourad Kaddiri. “Natural double-diffusive convection for the Carreau shear-thinning fluid in a square cavity submitted to horizontal temperature and concentration gradients.” *Journal of Non-Newtonian Fluid Mechanics* (2021).
- [75] Nag, Preetom and Md. Mamun Molla. “Non-Newtonian effect on double diffusive natural convection of nanofluid within a square cavity.” (2021).
- [76] Kolsi, Lioua, Shafqat Hussain, Kaouther Ghachem, Muhammad Jamal and Chemseddine Maatki. “Double Diffusive Natural Convection in a Square Cavity Filled with a Porous Media and a Power Law Fluid Separated by a Wavy Interface.” *Mathematics* (2022).
- [77] Arun, S. and A. Satheesh. “Mesoscopic analysis of MHD double diffusive natural convection and entropy generation in an enclosure filled with liquid metal.” *Journal of the Taiwan Institute of Chemical Engineers* (2019).
- [78] Sathiyamoorthi, Arun, Satheesh Anbalagan, Hakan F. Oztop and Nidal H. Abu-Hamdeh. “MHD Double-Diffusive Natural Convection in A Closed Space Filled with liquid metal: Mesoscopic Analysis.” *Applied and Computational Mechanics* (2020).